

Electronic Thesis and Dissertation Repository

---

6-6-2017 12:00 AM

## Dynamic Functional Connectivity Reveals Temporal Differences in Wake and Stage-2 Sleep

Mazen El-Baba, *The University of Western Ontario*

Supervisor: Dr. J Bruce Morton, *The University of Western Ontario*

Joint Supervisor: Dr. Adrian Owen, *The University of Western Ontario*

A thesis submitted in partial fulfillment of the requirements for the Master of Science degree in Neuroscience

© Mazen El-Baba 2017

Follow this and additional works at: <https://ir.lib.uwo.ca/etd>



Part of the [Cognitive Neuroscience Commons](#)

---

### Recommended Citation

El-Baba, Mazen, "Dynamic Functional Connectivity Reveals Temporal Differences in Wake and Stage-2 Sleep" (2017). *Electronic Thesis and Dissertation Repository*. 4603.

<https://ir.lib.uwo.ca/etd/4603>

This Dissertation/Thesis is brought to you for free and open access by Scholarship@Western. It has been accepted for inclusion in Electronic Thesis and Dissertation Repository by an authorized administrator of Scholarship@Western. For more information, please contact [wlsadmin@uwo.ca](mailto:wlsadmin@uwo.ca).

## Abstract

The transition from wakefulness to sleep is marked by changes in neurophysiology, suggesting that changes in consciousness might be accompanied by changes in functional network organization. Brain activity of 21 healthy participants was measured via simultaneous EEG-fMRI as participants transitioned from wakefulness into sleep. All fMRI volumes were ICA-decomposed, yielding 42 neurophysiological sources. Independent component time courses were used to estimate mean functional connectivity (FC) and dynamic FC using a sliding window technique. Windowed matrices were submitted to k-means clustering ( $k = 7$ , L2-norm). Mean FC in Wake and Stage-2 Sleep (S2S) were similar. Dynamic analysis revealed differences in temporal features of FC. Participants transitioned more between connectivity states (CSs) and spent less time across all CSs in Wake than in S2S. Four of the seven CSs differed in their frequencies. The current analysis suggests conventional FC analyses obscure features in FC that are observable on a finer temporal scale.

## Keywords

Sleep, Functional Connectivity, Dynamic FC, EEG-fMRI, Independent Component Analysis, k-means, Connectivity States.

## Acknowledgments

Dr. J Bruce Morton: I would like to deeply thank Dr. J Bruce Morton for his sincere care, thoughtfulness, supervision, and guidance. Dr. Morton, you have truly inspired me to strive for the best. Your academic and personal integrity truly reflect on the type of scholar, supervisor, and person you are. I am very fortunate to have had the opportunity to know you personally and professionally.

Ahmad El-Baba, Aseel El-Baba, Hadeel El-Baba, and Mayssa El-Bizri: your names were written alphabetically, so please do not complain about your position on the list. You are all always there for me no matter what. I could have never asked for a more supportive and loving family. You all mean so much to me. Mayssa and Hadeel, thank you for trying to listen to my talks. I know it probably felt like torture; but your willingness to hear them out means a lot to me. Aseel, you tried; and trust me, I understand that sleep is more important! Thank you for always pushing me to pursue my dreams. Also, I would like to send my special thanks to my mother, Mayssa, who was extremely helpful and supportive during the H.appi Camp. Without your help and support in everything I do, this Master's degree would not be possible.

Niki and Nellie Kamkar: thanking you for your love and care will never, ever, be enough. You were always there to make sure that my rainy days became sunny (with no chance of clouds).

Niki, thank you for the countless phone calls, random conversations, and advice. I always know that you have my back no matter what. I believe that I gained amazing colleagues, life-long friends, and family members!

Samantha Faith Goldsmith (SFG): My gut instinct almost never fails me... but I guess I have to admit, it did once! I am so grateful that you joined our lab in 2016. I can endlessly talk to you about anything! You were really my sanity check towards the end of my Master's journey. You were always there at the lab, and I was always happy to see you there! Sorry for placing you on the corner-desk of the lab!

Daniel J Lewis: I will never forget our long nights at the lab and our never-ending white-board drawings and discussions. You taught me so much in the past year and a half. I would still be fighting MATLAB right now if it was not for your generous help and patience!

Bea Goffin: I will deeply miss our "Bea chats". You have supported me in every step of the way. I can always walk in your office and spill my heart out knowing that you will be there to listen and support me in any way you can. For that, I thank you deeply!

Dr. Adrian Owen, Dr. Andrea Suddo, and Dr. Stuart Fogel: Thank you for your sincere care and for taking the time to advise me throughout my time at Western. I found our conversations extremely stimulating and enjoyable!

Dr. Stuart Fogel, Laura Ray, Lydia Fang, and Max Silverbrook: Thank you all very much for all your help. Our sleepless nights at the sleep lab (ironic) will never be forgotten!

# Table of Contents

Abstract.....	i
Acknowledgments.....	ii
List of Figures.....	vi
1.0 Introduction.....	1
1.1 A Historical Overview.....	1
1.1.2 Theological Account.....	1
1.1.1 Philosophical Account.....	2
1.2 Current Knowledge.....	3
1.3 Potential Caveats.....	6
2.0 Methods.....	8
2.1 Participants.....	8
2.2 Experimental Procedure.....	9
2.3 Data Acquisition and Preprocessing.....	9
2.4 Group ICA and Post-Processing.....	12
2.5 Stationary Mean FC Estimation.....	15
2.6 Dynamic FC Estimation.....	15
2.6 Dynamic Metrics.....	18
2.7 Reliability of Connectivity States and Dynamic Metrics.....	19
2.8 Estimating Heart Rate.....	19
3.0 Results.....	20
3.1 Stationary Mean FC.....	20
3.2 Dynamic FC.....	21
3.2.1 Connectivity States and Frequency.....	21

3.2.2 Mean Dwell Time .....	22
3.2.3 Reliability of Connectivity States and Dynamic Metrics .....	25
3.2.4 Temporal Characteristics of FC .....	28
3.2.5 Transition Probabilities .....	30
3.3 Heart Rate .....	31
4.0 Discussion .....	31
4.1 Mean vs. Dynamic FC .....	31
4.2 Theoretical Accounts .....	33
4.3 Connectivity States .....	35
4.4 Limitations .....	37
4.4.1 Stationary Analysis .....	37
4.4.2 Dynamic Analysis .....	38
4.4.3 Statistical Criteria .....	38
4.5 Concluding Remarks .....	39
References .....	40
Curriculum Vitae .....	56

## List of Figures

Figure 1. Step-by-step analysis steps are depicted in this figure. *A*, Subjects wake and sleep volumes were organized and submitted to group-level spatial independent component analysis (ICA). *B*, ICA was performed using the GIFT toolbox implemented in MATLAB; 42 neurophysiologically plausible sources were selected and sorted into functional families. GICA 1 back-reconstruction was used to estimate the time courses ( $R_i$ ) and spatial maps ( $S_i$ ) for each subject. *C*, All time courses (TCs) were post processed by removing subject motion variance, despiking, and filtering. *D*, TCs were used to estimate mean FC in Wake and Stage-2 Sleep by computing pairwise correlations between all ICs. *E*, As outlined by Allen et al., 2014, dynamic FC was estimated using a sliding window approach (window width = 15 TRs, time step = 1 TR) resulting in windowed correlation matrices. Correlation matrices were vectorized and concatenated into a large data matrix of all IC-to-IC pairwise correlation values over time. All windows were demeaned on a subject level by removing subject specific means from subject windows in Wake and Stage-2 Sleep. The concatenated data matrix was submitted to k-means clustering (*F*). k-means clustering was performed to extract recurrent features of the data. A k-7 solution was selected which resulted in a matrix with rows equivalent to the number of connectivity states (7) and columns equivalent to the number of unique IC-IC correlations (861). Each row representing a connectivity states was back-reconstructed into a matrix format to visualize coupling relationships between ICs. An IDX vector, a window state label vector, unique for each subject in Wake and Stage-2 Sleep was also computed revealing window classification under one of the 7 connectivity states..... 13

Figure 2. 42 neurophysiologically plausible independent components (ICs) were divided into groups and arranged based on their spatial and functional properties. A total of seven functional families were identified including the auditory, somatomotor, visual, default mode, cognitive control (including the dorsal and ventral attention networks), subcortical, and cerebellar networks. ICs are displayed on sagittal, coronal, and horizontal slices on a cortical surface implemented in MANGO. .... 17

Figure 3. Mean functional connectivity in WAKE (A), and STAGE-2 Sleep (B). Each square represents the coupling relationship between the IC on the x-axis and the IC on the y-axis. The diagonal represents a perfect ( $r = 1.0$ ) correlation between an IC and itself. Within defined boundaries around the diagonal, positive correlations were found indicating strong coupling relationships between ICs that were classified under the same functional family (e.g., ICs within the Auditory network). Off-diagonally, weaker connectivity can be found between functional families..... 20

Figure 4. Stationary Mean FC in Wake (B) subtracted from stationary mean FC in Stage-2 Sleep (A) to produce a Difference Matrix (C). *t* tests were performed with the null hypothesis of zero correlation on the Difference Matrix (D). To correct for multiple comparisons, the false discovery rate (FDR) method was used with a *P* value of .01. *t*-tests confirmed that mean FC in Wake and Stage-2 Sleep were similar, as differences between the correlations in both conditions were not significantly greater than 0..... 21

Figure 5. IDX vector of three representative participants during wakefulness. The number of windows is on the x-axis and the connectivity state is on the y-axis. Plots illustrate transitions between connectivity states. The IDX vector was used to derive dynamic metrics. .... 23



Figure 6. Clustering analysis revealed 7 connectivity states in Wake and Stage-2 Sleep (A). Each square represents the coupling relationship between the IC on the x-axis and the IC on the y-axis. B, mean frequency of state expression in Wake (yellow) and Stage-2 Sleep (blue). The frequency of connectivity state-1 and 6 were significantly greater in Stage-2 Sleep (\*,  $p < .05$ ). The frequency of connectivity state-5 was significantly greater in Wake (\*,  $p < .05$ ); the frequency of connectivity state-4 expression in wake was marginally significant when compared to Stage-2 Sleep (#,  $p = .053$ ). C, mean dwell time of the four connectivity states that had differences in their frequencies of expression in Wake and Stage-2 Sleep. Mean dwell time was significantly greater in Stage-2 Sleep than in Wake (\*,  $p < .05$ )..... 24

Figure 7. Spatial correlations comparing connectivity states from a k-5 solution and k-7 solution. Black lines connect qualitatively similar connectivity states. Red dashed lines show the spatial correlations of connectivity state-1 in a k-5 solution with connectivity states in a k-7 solution. Weaker correlations are indicative of the robustness of the connectivity states in varying k-solutions and the uniqueness of their spatial topologies. Spatial correlations were iteratively computed between all connectivity states to confirm the similarity of selected connectivity states across varying k-solutions..... 26

Figure 8. Difference scores were computed for connectivity states that showed statistically significant differences in Wake and Stage-2 Sleep. Top three panels show the connectivity states matrices derived from k-5, k-7, and k-15 solutions. The connectivity states were organized by grouping, column-wise, qualitatively similar states. Each group is highlighted and labeled as A, B, or C. Corresponding bar graphs are also labeled and highlighted with the same colour. The frequency of expression for connectivity state-1 (A), connectivity state-5 (B), and connectivity state-6 (C) in a k5 and k15 solution was subtracted from a k7 solution frequency score. Yellow

bars represent the difference scores during Wake, and blue bars represent the difference scores in Stage-2 Sleep. Frequency of expression did not change across k-solutions. This is indicative of the robustness of the dynamics analysis across different k solutions. .... 27

Figure 9. Mean number of transition (NT) in Wake and Stage-2 Sleep. Participants' NTs in Wake and Stage-2 Sleep are transformed by dividing their NT by the length of their IDX vector. Participants expressed more transitions in Wake than in Stage-2 Sleep ( $p < .05$ ). .... 29

Figure 10. Mean inter-transition interval (average number of consecutive windows) in Wake and Stage-2 Sleep. Y-axis represents the number of consecutive windows. The inter-transition interval was significantly higher in Stage-2 Sleep than in Wake ( $p < .05$ ). .... 29

Figure 11. Transition probabilities for Stage-2 Sleep and Wake shown. Matrices represent the probability of transitioning from i-state on the y-axis to j-state on the x-axis. Darker yellow squares in the Difference matrix represent a higher probability of transition in Stage-2 Sleep than Wake, while darker blue squares represent a higher probability of transition in Wake than Stage-2 Sleep. Probabilities in the difference matrix range from 0 to .10. .... 30

Figure 12. Mean heart rate (beats per minute) in Wake and Stage-2 Sleep. There was no difference in heart rate between conditions. .... 31

## 1.0 Introduction

### 1.1 A Historical Overview

#### 1.1.2 Theological Account

Over the past centuries, many scholars, philosophers, and religious leaders asked questions related to sleep. According to Middle Eastern folktales, sleep is an intermediate state between wakefulness and death. It is regarded as the gateway for the living to interact with the dead. These ideas are instantiated in religious scriptures that discuss the role of the *soul* in the transition from wakefulness to sleep. In Islam, death and sleep are often discussed in the same verses of the Qur'an (BaHammam, 2011). The holy book of Islam states that God (Allah) takes the human *soul* permanently upon death, but retains the *soul* only temporarily during sleep (BaHammam, 2011). It is said that the soul exits the body through a person's navel, allowing the *soul* to venture between the living and the dead. Accordingly, dreams that include alive and deceased individuals are thought to be a result of the souls communicating with one another during sleep. Because sleep is regarded as an intermediary stage, when the Prophet Mohammed was asked if people sleep in Heaven, he answered: "*sleep is the brother of death. People of Heaven do not sleep*" (BaHammam, 2011). His statement indicates that once a person is dead, they will no longer be able to sleep because they will be living, awake, eternally in Heaven.

The comparison of sleep and death predates Islam as parallels are also drawn in the Old and the New Testaments. Sleeping and dying appear to be synonymous in Christian Holy books. For instance, Jesus informed his disciples that Lazarus of Bethany "has fallen asleep" and later

reiterated his statement by saying “Lazarus is dead” (Jn. 11:14). Perhaps, sleep and death were viewed under the same lens given the similarity of the body’s appearance in both states—immobile and unaware. In Judaism, sleep is considered 1/60<sup>th</sup> of death. Like Muslims, Jews believe that the soul is taken and cleansed by God during sleep, and is returned to the human body upon wakefulness. For that reason, Jews and Muslims, alike, recite a prayer upon waking, thanking God for restoring their souls. For example, the Jews say: “I offer thanks to You, living and eternal King, for You have mercifully restored my soul within me; Your faithfulness is great.”

### 1.1.1 Philosophical Account

Alcmaeon (450 BC) was one of the earliest Greek philosophers on record to propose that the flow of blood from the skin to the core was essential in mediating the transition from wakefulness to sleep, whereas the outward flow of blood towards the skin would result in wakefulness (Papachristou, 2014). A century later (350 BC), Aristotle continued the quest to unravel the mystery of sleep by proposing that sleep occurs during the process of digestion, and ceases when digestion is complete (Papachristou, 2014). These philosophical ideas are indicative of the dominant school of thought during ancient times that focused on the heart and the blood to explain changes in conscious experience. Aristotle postulated that the heart was the origin of nerves and was responsible for human intelligence, sensation, and emotion. These ideas were predominant until the mid-seventeenth century; however, the notion that sleep is associated with a change in consciousness was first instantiated by Galen (162 BC), who deduced that if consciousness resides in the brain and sleep is an attenuation of consciousness, then sleep must be due to changes in brain function.

These philosophical and theological accounts have influenced cultural folktales and stories that attempt to explain the importance of sleep. Interestingly, parallels can be drawn between theological accounts and knowledge obtained from recent studies. For instance, the Jewish account, stating that the soul is taken and cleansed by God during sleep, is reminiscent of the restorative effects of sleep discussed in current literature (e.g., Poe, 2017; Xie et al., 2013). These ancient accounts are a testament of the deeply rooted interest in understanding questions relating to sleep. The human fascination with sleep is not surprising given that humans spend a third of their lives sleeping; without it, they would die. With current cutting-edge technology, researchers are just beginning to unravel the mysteries behind sleep. Perhaps, answering questions related to the involvement of the *soul* during the transition from wakefulness to sleep is not possible; however, many advancements have been made using neuroimaging technology that reveal neurophysiological changes that occur during this transition.

## 1.2 Current Knowledge

The transition from wakefulness to sleep is accompanied by widespread changes in brain function that impact learning (Yang et al., 2014), memory (Diekelmann & Born, 2010; Maingret, Girardeau, Todorova, Goutierre, & Zugaro, 2016), attention (Kirszenblat & van Swinderen, 2015), immunity (Irwin & Opp, 2016), and overall health (Luyster, Strollo, Zee, & Walsh, 2012). This transition is also marked by a change in conscious state (Diering et al., 2017). Functional changes in altered states of consciousness can be examined microscopically – on a molecular and cellular level – revealing changes in synaptic modulation throughout sleep-wake cycles (Diering et al., 2017). They can also be examined macroscopically (i.e., on a functional network or whole-brain level; Tagliazucchi, Behrens, & Laufs, 2013), revealing a breakdown of cortical effective connectivity (Massimini et al., 2005) — the causal impact of neuronal groups on the firing of

other neuronal groups (Lee, Harrison, & Mechelli, 2003). These changes in brain function have profound restorative effects on brain function by clearing neurotoxic build-up (Xie et al., 2013), removing “unnecessary” information (Poe, 2017), and allowing for synaptic plasticity to occur (Tononi & Cirelli, 2014).

Through the use of imaging methods, such as simultaneous electroencephalogram and functional magnetic resonance imaging (EEG-fMRI), researchers have examined changes in the spatial organization of functional brain networks during the transition from wakefulness to sleep. Using the stationary mean functional connectivity (FC) approach, pairwise correlations between the blood oxygenated level dependent (BOLD) time courses of nodes — brain regions of interest — are computed, thus elucidating spatial features of network connectivity (Ferrarelli et al., 2010; Fox et al., 2005; Greicius, Krasnow, Reiss, & Menon, 2003; Rissman, Gazzaley, & D’Esposito, 2004). During wakefulness or while “resting”, brain networks assume spatial organizations that form spontaneously (Biswal, FZ, VM, & JS, 1995; de Pasquale et al., 2010, 2012; Fox & Raichle, 2007; Fox et al., 2005; Fransson, 2005; Greicius et al., 2003; Raichle & Mintun, 2006; Rogers, Morgan, Newton, & Gore, 2007; Vincent et al., 2007). In contrast, the descent into sleep is marked by a breakdown in network connectivity (Boly et al., 2009; Gustavo Deco, Hagmann, Hudetz, & Tononi, 2014; Horovitz et al., 2009; Sämann et al., 2011; Tagliazucchi, von Wegner, et al., 2012) that is characterized by a shift from a globally integrated network to discrete local sub-networks (Boly et al., 2012; Gustavo Deco et al., 2014; Godwin, Barry, & Marois, 2015a; Spoormaker et al., 2010; Spoormaker, Gleiser, & Czisch, 2012). In particular, coupling between the anterior and posterior nodes of the default mode network (DMN) have been linked to the sustenance of conscious awareness during wakefulness (Horovitz et al., 2009; Sämann et al., 2011); however, these changes have not been consistently detected (Larson-Prior et al., 2009).

The role of the DMN has also been examined in patients suffering from disorders of consciousness. Patients in the vegetative state (VS), a consciousness state characterized by normal sleep-wake cycles but a lack of awareness, showed a left lateralized DMN as right regions of the network had reduced connectivity (Cauda et al., 2009). However, these findings are not reliability reported as other evidence shows a global reduction in connectivity of the DMN in VS patients (Boly et al., 2009). Although these findings discuss a fundamentally different conscious and behavioural state (i.e., vegetative state), they call into question the reliability of the analytical methods used in elucidating features of FC that may distinguish between these states.

Considering that the descent from wakefulness to sleep has a global impact on neurophysiological function, changes in features of FC must impact whole-brain network. A macroscopic inspection of network connectivity has revealed that the brain's functional and structural connectivity increase in their similarity with an attenuation of conscious awareness (Tagliazucchi, Crossley, Bullmore, & Laufs, 2016). Similarly, the topology of the FC repertoire of the brains of anesthetized primates closely resembles the brain's structural connectivity. In contrast, during wakefulness, the topological organization of functional networks markedly depart from the brain's structural connectivity (Barttfeld, Uhrig, Sitt, Sigman, & Jarraya, 2015). However, functional connectivity patterns during rest (i.e., wakefulness) have also been shown to reflect the brain's structural connectivity (Greicius, Supekar, Menon, & Dougherty, 2009). The resemblance of the brain's functional and structural connectivity during rest is argued to aid in the brain's ability to integrate functional information and bring about conscious experience (Hagmann et al., 2008).

### 1.3 Potential Caveats

Whether conventional stationary FC methods fully characterize differences in brain connectivity that occur in the transition from wake to sleep is unclear. Conventional methods assume a stable connectivity architecture over time or throughout an imaging period (Hutchison et al., 2013), obscuring temporal features that may distinguish between FC in wakefulness and sleep. Investigating changes in stationary mean FC across consciousness states allows for an examination of how spatial couplings between functionally connected networks (Ferrarelli et al., 2010; Godwin, Barry, & Marois, 2015b), or within a network change. However, little is known about how temporal features of brain function change from wakefulness to sleep, and whether such changes can be observed on a whole-brain level.

Emergent evidence highlights that the brain is functionally dynamic (Allen, Eichele, Wu, & Calhoun, 2017; Hansen, Battaglia, Spiegler, Deco, & Jirsa, 2015; Hutchison & Morton, 2015; Hutchison & Morton, 2015; Kiviniemi et al., 2011), given that functional connections exhibit transient changes that impact the coupling relationship of canonical brain networks (Chang et al., 2013; Handwerker, Roopchansingh, Gonzalez-Castillo, & Bandettini, 2012; Kiviniemi et al., 2011; Smith et al., 2012; Tagliazucchi, Wegner, et al., 2012; Tagliazucchi, Balenzuela, Fraiman, & Chialvo, 2012). These transient characteristics of FC are indicative of transitions between different connectivity states (FC states that have unique spatial topologies). Brain transitions allow for flexible switching between connectivity states in order for the brain to meet its cognitive demands and to attend to the external environment (Chang & Glover, 2010; Handwerker et al., 2012; Smith et al., 2012). If there were differences in the number of state transitions between different conscious states, then the average time that the brain is spending across connectivity states would also be different. Transient coupling between connectivity



networks accompanies changes in conscious and cognitive states (for review see Hutchison et al., 2013), as well as, changes within states (e.g., during rest) (Hutchison et al., 2012). These observations support the argument that functional connections in the brain are not static; but are indeed, dynamic.

As previously demonstrated, stationary mean FC is limited in characterizing differences between different vigilant conditions (i.e., eyes open versus eyes closed) (Allen et al., 2017). Using simultaneous EEG/ fMRI and dynamic FC methods, connectivity states were expressed in each vigilant condition that were marked by unique coupling relationships between functional networks (Allen et al., 2017). Further, similar connectivity states were expressed across both conditions, indicating that a mean FC characterization of each condition may not be sufficient at revealing features of FC that may differentiate between each vigilant condition (Allen et al., 2017). Given the theoretical framework that discuss spatio-temporal changes in FC across changes in consciousness states (Tononi, 2004; Tononi, Boly, Massimini, & Koch, 2016) and evidence that support it (Kannurpatti, Biswal, Kim, & Rosen, 2008; Pillow et al., 2008; Schroter et al., 2012), an investigation of temporal features of FC is warranted.

In this study, stationary and dynamic FC in wake and sleep were investigated on a whole-brain level. To this end, stationary mean FC in wakefulness and sleep was compared. Then, temporal features of FC were examined. Given evidence that shows a breakdown in cortical effective connectivity that impacts the spatiotemporal propagation of neuronal activity (Massimini et al., 2005, 2010), then temporal characteristics of FC that differentiate wakefulness from sleep were expected to be observed. Dynamics FC was predicted to differentiate between wakefulness and sleep more than the conventional mean FC method. *A Slow Sleep Brain (SSB) Hypothesis* was proposed that predicts slower brain dynamics in sleep when compared to

wakefulness that will impact the brain's dwell time while in a FC state and its frequency of expression of such states. Evidence showing changes in dynamic FC may provide important biomarkers for changes in conscious state and may reveal important features of brain function that allow sleep to have such profound restorative effects.

## 2.0 Methods

### 2.1 Participants

Thirty-six healthy right-handed adults [20 female, ages 20- to- 25 years ( $M = 25.6$ ,  $SD = 3.6$ )] were recruited to participate in this study. All participants were screened according to the following exclusion criteria, including, non-shift workers, no history of head injury or seizures, a normal body mass index ( $< 25$ ), medication-free, and no excessive caffeine, nicotine, or alcohol consumption. Furthermore, participants were required to meet the MRI safety screening criteria. Participants who passed the initial screening were then assessed using psychopathology questionnaires. Participants had to score 10 or lower on the Beck Depression (Beck, Steer, & Garbin, 1988; Beck, Rial, & Rickels, 1974) and the Beck Anxiety (Beck, Epstein, Brown, Steer et al., 1988); as well, participants demonstrated no history or signs of sleep disorders as measured using the Sleep Disorders Questionnaire (Douglass et al., 1994). Participants were asked to comply with a strict sleep schedule for seven days prior to scanning that required them to maintain regular sleep-wake cycles (i.e., sleep-time between 22h00 and 24h00, and wake-time between 07h00 and 09h00), and to refrain from taking day-time naps. Participants were instructed to complete a sleep diary detailing their consumption of stimulants (e.g., caffeine) and their sleep/wake times. Wrist actigraphy (Actiwatch 2, Philips Respironics, Andover, MA, USA), worn on the non-dominant wrist, were used to assess compliance to the sleep schedule.

All participants provided written informed consent and were financially compensated. The Western University Health Science Research Ethics Board provided ethics approval for this study.

## 2.2 Experimental Procedure

All participants were screened at least one week before scanning. Participants were then invited to the laboratory two hours prior to data acquisition. During the two hours, participants were briefed on the procedures and were given the study's letter of information to obtain informed consent. Electrocardiogram (ECG) electrodes were first positioned around the thoracic cavity. EEG caps were then positioned on the head. Electrical impedances were measured to ensure that the ECG and EEG electrodes were well-positioned and were functioning properly. Imaging procedures occurred between 21h00 and 23h00. Simultaneous EEG-fMRI data was recorded while participants were instructed to remain awake in the scanner for the wake session (8 min, 32 s), and then were asked to sleep until awoken at the end of the scanning time. Participants were then accompanied to the Sleep Lab, where they spent the remainder of the night.

## 2.3 Data Acquisition and Preprocessing

A 3.0T Magnetom Prisma magnetic resonance imaging system (Siemens, Erlangen, Germany) and a 32-channel radio frequency head coil were used to acquire imaging data. At the beginning of the scan, a structural T1-weighted image was acquired using a 3D MPRAGE sequence with TR = 2300 ms, TE = 2.98 ms, TI = 900 ms, FA = 9°, 176 slices, FoV = 256 mm x 256 mm, matrix size = 256 x 256, yielding a voxel size 1 mm x 1mm x 1mm. T2\*- weighted

functional images were acquired during wake and sleep sessions with a gradient echo-planar sequence using axial slice orientation with TR = 2160 ms, TE = 30 ms, FA = 90°, 40 transverse slices, 3 mm slice thickness, 10% inter-slice gap, FoV = 220 mm x 220 mm, matrix size = 64 x 64, yielding a voxel size = 3.44 mm x 2.44 mm x 3 mm. The aforementioned sequence parameters were chosen to allow for simultaneous EEG recording with a time stabilized gradient artifact, and to ensure that the gradient artifact harmonic (18.52 Hz) would not interfere with the spindle band frequency (11 – 16 Hz). A 2160 ms repetition time was chosen to match EEG sample time (common multiple of 0.2 ms), scanner clock precision product (0.1  $\mu$ s), and the total number of slices (40) used (Multert & Lemieux, 2009).

Functional images were preprocessed using SPM12 (<http://www.fil.ion.ucl.ac.uk/spm/software/spm12/>) in MATLAB (version 9.6.1 R2016b). Standard preprocessing procedures included realignment using rigid body transformations and reslicing; coregistration of the mean realigned image to the structural T1-image; spatial normalization of the resultant volumes into Montreal Neurological Institute (MNI152) space; and smoothing with a Gaussian kernel (FWHM = 8 mm).

A 64-channel magnetic resonance (MR) compatible EEG cap [including one ECG lead, Brain MR, EasyCap, Herrsching, Germany] and two MR-compatible 32-channel amplifiers (Brainamp MR plus, Brain Products GmbH, Gliching, Germany) were used to acquire simultaneous EEG during the scanning session. Participants' heads were cushioned using comfortable foam to restrict head movements in the scanner and to reduce motion-related EEG and fMRI artifacts. Scalp electrodes were referenced to FCz, and two bipolar ECG recordings from V2 – V5 and from V3 – V6 using an MR-compatible 16-channel bipolar amplifier (Brainamp ExG MR, Brain Products GmbH, Gliching, Germany). Electrode-skin impedance was

reduced to  $< 5$  kOhm using high-chloride abrasive electrode paste (Abralyt 2000 HiCL; EasyCap, Herrsching, Germany).

EEG was acquired at a 5000 samples per second rate and was digitized with a 500-nV resolution. An analog filter using a band-limited low pass filter (500 Hz) and a high pass filter (10 s corresponding to 0.0159 Hz) was applied on EEG data. A fiber optic cable transferred EEG and ECG recordings to a personal computer that was synchronized to the scanner's clock using a Brain Products Recorder Software, Version 1.0x (Brain Products, Gilching, Germany). Online monitoring of EEG was performed using Brain Products RecView software to correct for online artifacts.

Standard sleep stage scoring was performed (Silber et al., 2007) using the VisEd Marks toolbox ([https://github.com/jadesjardins/vised\\_marks](https://github.com/jadesjardins/vised_marks)) in EEGLAB (Delorme & Makeig, 2004). A validated automatic spindle detection method was performed (Albouy et al., 2013; S. M. Fogel et al., 2014; S. Fogel, Ray, Binnie, & Owen, 2015; Ray et al., 2015) using EEGLAB-compatible software that runs through MATLAB (Delorme & Makeig, 2004) ([github.com/stuartfogel/detect\\_spindles](https://github.com/stuartfogel/detect_spindles)). Fz, Cz, and Pz derivations were used to detect spindles, a marker of Stage-2 sleep, after the EEG data was down-sampled to 250 Hz. A complex demodulation transformation of the EEG signal (bandwidth = 5 Hz) with a carrier frequency centered on 13.5 Hz (Iber et al., 2007) was performed. Refer to Ray et al. (Ray et al., 2015) for more details regarding processing steps and procedures. In all, EEG data processing was utilized to classify different sleep stages [i.e., non-rapid eye movement sleep (NREM) Stage-1, -2, and slow-wave sleep (SWS) Stage-3].

## 2.4 Group ICA and Post-Processing

An overview of the analysis is depicted in **Figure 1**. Of the 36 participants, 21 were included in the analysis who had sufficient sleep volumes (i.e., a minimum of 5 minutes of consolidated sleep volumes), and whose volumes were not contaminated by motion artifacts (translation cutoff = 1.5mm, rotation cutoff = 1.5 degrees). Sleep stage onsets and durations were computed using EEG data to separate functional volumes acquired during the sleep session into Wake, Stage-1 [non-rapid eye movement (NREM) sleep-1], Stage-2 (NREM-2), Stage-3 (slow wave sleep), and REM sleep for subsequent analyses. Participants had an average of 419 volumes classified under Stage-2 sleep. Only seven participants had sufficient volumes in Stage-3 sleep; thus, in an effort to maximize statistical power, dynamics analyses were confined to data from Wake and Stage-2 Sleep.

All wake and sleep volumes were submitted to a group-level spatial ICA implemented in the GIFT toolbox (<http://mialab.mrn.org/software/gift/>) in MATLAB to decompose data into functional networks. In the first step, Principal Components Analysis (PCA) reduces subject-specific data to 65 components. The Infomax algorithm was then applied to obtain 65 maximally independent components (ICs). A high order model was used to optimally separate noise and source components, as well, to ensure a spatially fine-grained parcellation of cortical and subcortical brain regions (Abou-Elseoud et al., 2010; Kiviniemi et al., 2009; Smith et al., 2009). Subject ICs were then back reconstructed. Of the 65 ICs, 42 were identified as neurophysiological plausible (see **Figure 2**) by two observers based on an independent visual inspection of the spatial maps. The 42 ICs were classified under seven functional networks that include the subcortical (SC), auditory (AUD), somatomotor (SM), visual (VIS), cognitive control

(CC) [including dorsal attention (DA) and ventral attention (VA)], default mode (DMN), and cerebellar (CB) network (**Figure 2**).

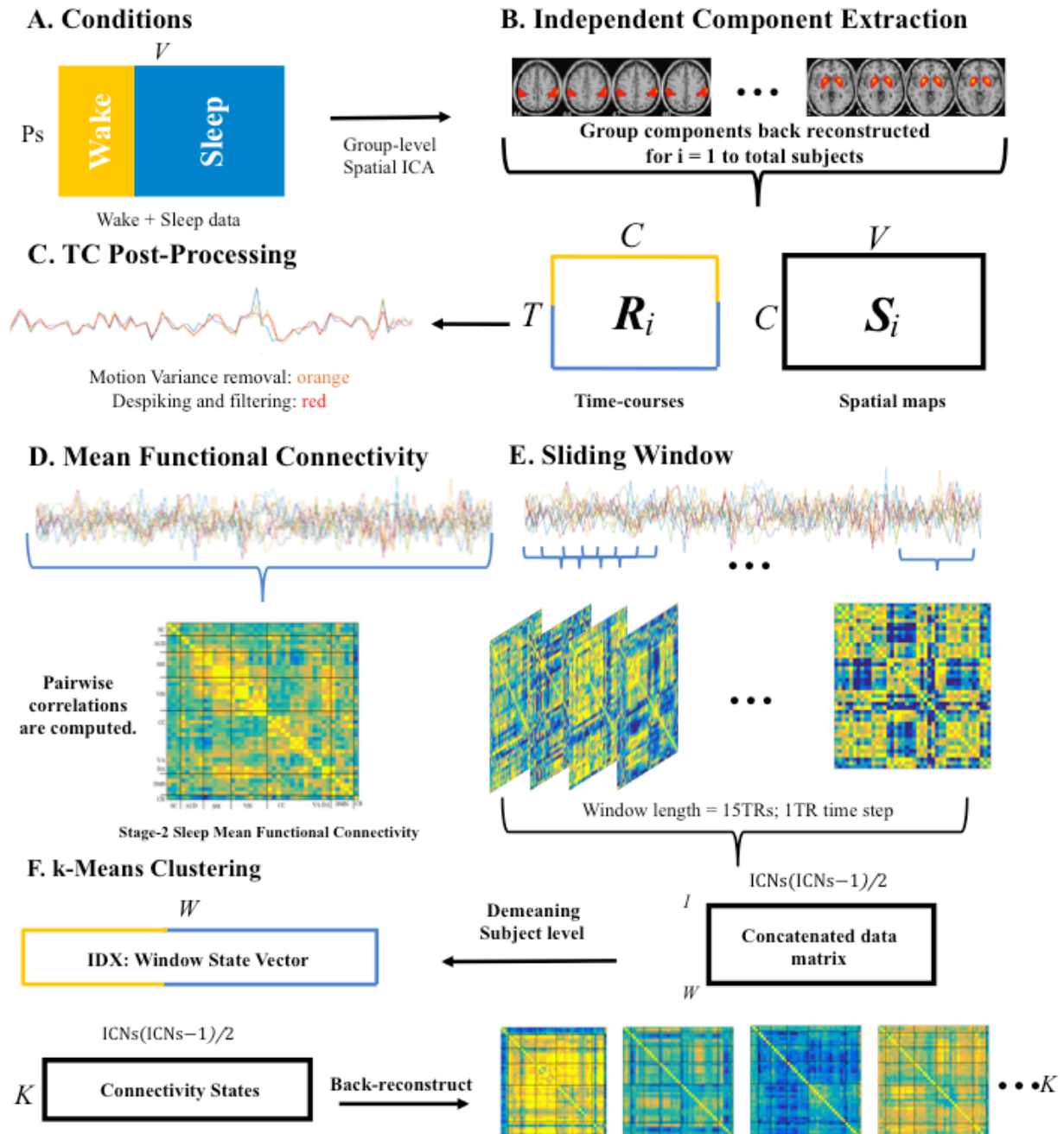


**Figure 1.** Step-by-step analysis steps are depicted in this figure. *A*, Subjects wake and sleep volumes were organized and submitted to group-level spatial independent component

analysis (ICA). *B*, ICA was performed using the GIFT toolbox implemented in MATLAB; 42 neurophysiologically plausible sources were selected and sorted into functional families. GICA 1 back-reconstruction was used to estimate the time courses ( $R_i$ ) and spatial maps ( $S_i$ ) for each subject. *C*, All time courses (TCs) were post processed by removing subject motion variance, despiking, and filtering. *D*, TCs were used to estimate mean FC in Wake and Stage-2 Sleep by computing pairwise correlations between all ICs. *E*, As outlined by Allen et al., 2014, dynamic FC was estimated using a sliding window approach (window width = 15 TRs, time step = 1 TR) resulting in windowed correlation matrices. Correlation matrices were vectorized and concatenated into a large data matrix of all IC-to-IC pairwise correlation values over time. All windows were demeaned on a subject level by removing subject specific means from subject windows in Wake and Stage-2 Sleep. The concatenated data matrix was submitted to k-means clustering (*F*). k-means clustering was performed to extract recurrent features of the data. A k-7 solution was selected which resulted in a matrix with rows equivalent to the number of connectivity states (7) and columns equivalent to the number of unique IC-IC correlations (861). Each row representing a connectivity states was back-reconstructed into a matrix format to visualize coupling relationships between ICs. An IDX vector, a window state label vector, unique for each subject in Wake and Stage-2 Sleep was also computed revealing window classification under one of the 7 connectivity states.

IC time courses (TCs) were then further post-processed to retain maximal signal-to-noise ratio. First, estimates of translational and rotational motion were regressed out of individual TCs using linear regression. Second, resultant residuals were filtered using a Butterworth filter, and TCs were despiked by replacing any spike greater than 3 standard deviations (STDV) with values equal to 3 STDV. Last, a Fisher z-transformation was applied, and the resultant TCs were used for further analyses.



## 2.5 Stationary Mean FC Estimation

Each condition,  $c$ , and a correlation matrix  $C_c$ , was estimated to visualize and compare stationary connections in Wake and Stage-2 Sleep. Full time courses of all 42 ICs for each subject ( $s$ ) were cross-correlated to compute stationary mean FC in Wake and Stage-2 Sleep. Each matrix had 861 unique comparisons. Group stationary mean FC in Wake and Stage-2 Sleep were then computed by taking the average cross-correlations across subjects. Stationary FC in Wake and Stage-2 Sleep were assessed based on their similarity. Furthermore, to better visualize stationary FC differences across conditions, a difference matrix was computed ( $C_{\text{Stage-2 sleep}} - C_{\text{Wake}}$ ). To test for statistical significance of connectivity between ICs,  $t$  tests were performed on all unique elements of the difference matrix with the null hypothesis of zero correlation. To correct for multiple comparisons, the false discovery rate (FDR) method was used with a  $P$  value of .01.

## 2.6 Dynamic FC Estimation

Following the procedure of Allen et al. (2014), dynamic FC was estimated using a sliding window method. Pearson correlation matrices were computed from windowed segments (window width = 15TRs, time step = 1TR) of IC time courses, separately for Wake and Stage-2 Sleep data. The window width was selected based on empirical precedence (Allen et al., 2014). Resultant window ( $W$ ) matrices had 861 features representing the total number of unique elements ( $uE$ ,  $n(n-1)/2$ ), such that each element ( $e$ ) represents a temporal correlation between two ICs. All windows across subjects and condition were concatenated into a matrix composed of rows equal to total number of windows and columns equal to  $uE$  ( $W_{\text{total}} \times uE = 23,649 \times 861$  that include 4186 Wake  $W$ s, 3379 Wake  $W$ s during sleep session, 932 Stage-1 Sleep  $W$ s, 12,175

Stage-2 Sleep Ws, and 2977 Stage-3 Sleep Ws). Windows obtained did not run between stages of sleep. Windows were concatenated based on time courses obtained from each sleep stage. Windows were demeaned on a subject level by calculating the subject's mean and subtracting the mean from each window. Demeaning was performed to observe dynamic fluctuations outside of the mean. IC-IC couplings that participants express during Wake and Stage-2 Sleep characterize these dynamic fluctuations.

The resultant matrix was then submitted into a k-means clustering algorithm in order to find recurring whole-brain FC configurations (Lloyd, 1982) across all participants in wake and sleep. The squared Euclidean distance metric was used to evaluate distances between windowed correlation matrices. k-means clustering was computed with k-solutions ranging from 2 to 21. To choose a k-solution for subsequent dynamic analysis, all connectivity matrices derived from the clustering analysis were qualitatively assessed. An increase in the number of connectivity states resulted in connectivity states that resembled one another, while a k-7 solution revealed qualitatively unique connectivity states. Therefore, a k-7 solution was chosen for further dynamics analyses (Allen et al., 2014; Barttfeld et al., 2015). This qualitative assessment was quantitatively analyzed to assess the robustness of the connectivity states that are observed and to ensure that the k-means solution does not bias the dynamics results.

k-means clustering produces two outcomes of interest that were used to compute dynamic metrics. First, a C-matrix composed of k-rows and columns equal to the number of unique elements in the FC matrices was generated. Each row represents a connectivity state that was identified by k-means as a recurrent pattern in the data. Second, an IDX vector, or a window state label vector, is generated that classifies each window as an instance of a connectivity state.

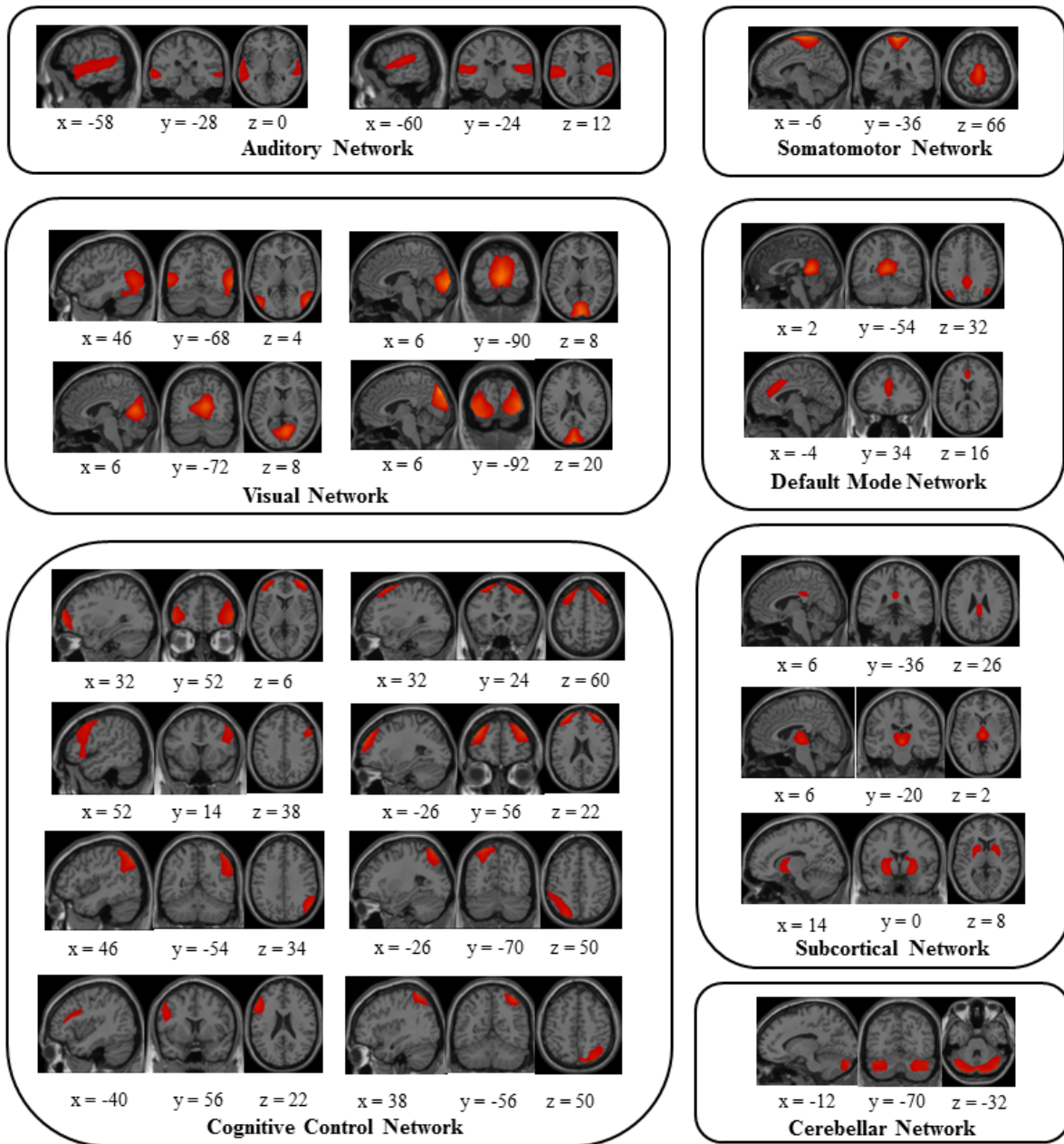


**Figure 2.** 42 neurophysiologically plausible independent components (ICs) were divided into groups and arranged based on their spatial and functional properties. A total of seven functional families were identified including the auditory, somatomotor, visual, default mode, cognitive control (including the dorsal and ventral attention networks), subcortical, and cerebellar networks. ICs are displayed on sagittal, coronal, and horizontal slices on a cortical surface implemented in MANGO.

## 2.6 Dynamic Metrics

To characterize temporal changes in inter-network functional connectivity, and to compare connectivity dynamics across wake and sleep, the IDX vector was parsed into subject-specific segments, and then further parsed into separate wake and sleep state label vectors. The longest consecutive chain(s) of windows present per participant were used to preserve temporal features of the data ( $M = 307$ ,  $SD = 259$  consecutive windows). Resulting vectors were used to compute five dynamic metrics, separately for subjects and conditions (i.e., wake and sleep), including: (1) frequency (F) measured as the proportion of all windows classified as instances of a particular state, and computed separately for each state; (2) mean dwell time (MDT), measured as the average number of consecutive windows classified as instances of the same state, and computed separately for each state; (3) the number of transitions (NT), measured as the number of state transitions; (4) inter-transition interval (ITI), measured as the average number of consecutive instances of a state before a transition to a different state, computed as an average across all states; and (5) transitional probability, measured as the probability of transitioning from connectivity State X to connectivity State Y. To compute NT, participant averages were transformed by dividing the total number of transitions by the total length of the IDX vector used with consecutive window labels. The transformation step was necessary to ensure that NT was not biased by the length of the IDX vector, given the length of the IDX vector for the sleep condition varied across participants.

$$FSE_k = \frac{W_k}{total\ W}$$

$$MDT_k = \mu_{Wk}$$

$$NT_{condition} = \mu(transitions)$$

$$ITI_{condition} = \sum_{i=1 \rightarrow W} \frac{length(W)}{nW}$$

## 2.7 Reliability of Connectivity States and Dynamic Metrics

The reliability of the connectivity states was assessed by computing spatial correlations between connectivity states obtained from the k-7 solution and states from varying k-values (2 to 21). Further, spatial correlations were iteratively calculated between all connectivity states to show that only qualitatively similar states were highly correlated, while qualitatively dissimilar states were weakly correlated.

The difference of the states' frequencies in a k-7 and k-x solution was also computed to assess the robustness of the dynamic metric across varying k-values. Difference scores were computed on the frequencies of expression for states that showed significant differences in Wake and Stage-2 Sleep in a k-7 solution. Difference scores were statistically assessed using Repeated Measures ANOVA for comparisons between 2 or more difference scores and paired t-test for a single comparison.

## 2.8 Estimating Heart Rate

Using the participants' ECG data, heart rate was estimated by computing the R-R interval during Wake and Stage-2 Sleep. Because there were various durations and onsets of Stage-2 Sleep across participants, average heart rate throughout all Stage-2 sleep was computed for each participant.

## 3.0 Results

### 3.1 Stationary Mean FC

Stationary mean FC in Wake and Stage-2 Sleep were estimated by computing pairwise correlations between the TCs of the 42 ICs from both conditions. Resulting FC matrices were highly similar (spatial correlation;  $r = .865, p < .001$ ; **Figure 3**), and marked by weak positive and negative inter-network correlations and positive intra-network correlations. To test for differences, each participant's Wake matrix from their Stage-2 Sleep matrix were subtracted, and tested resulting differences against 0 at the group level by means of  $t$  tests corrected for multiple comparisons using the false discovery rate (FDR) method ( $P .01$ , **Figure 4**). No differences were significantly different than 0.

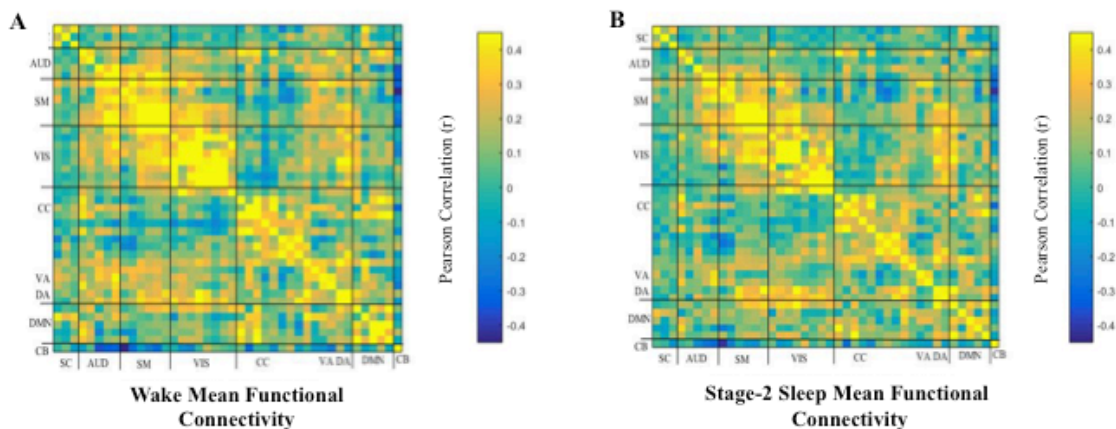


**Figure 3.** Mean functional connectivity in WAKE (A), and STAGE-2 Sleep (B). Each square represents the coupling relationship between the IC on the x-axis and the IC on the y-axis. The diagonal represents a perfect ( $r = 1.0$ ) correlation between an IC and itself. Within defined boundaries around the diagonal, positive correlations were found indicating strong coupling relationships between ICs that were classified under the same

functional family (e.g., ICs within the Auditory network). Off-diagonally, weaker connectivity can be found between functional families.

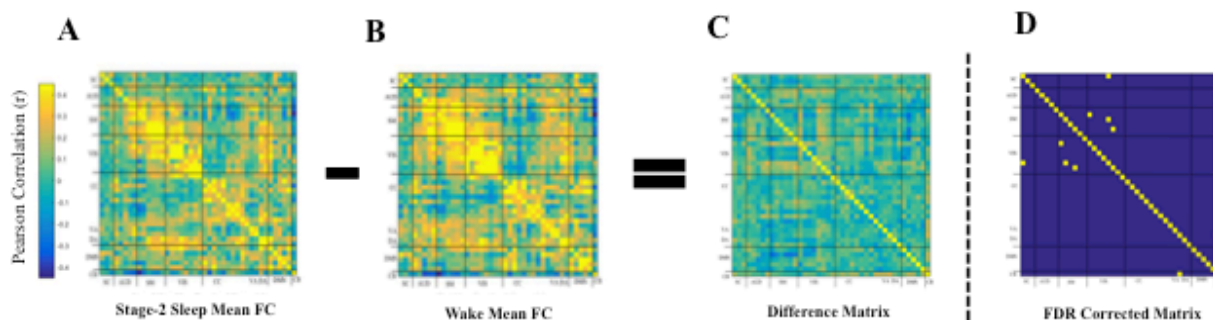


**Figure 4.** Stationary Mean FC in Wake (B) subtracted from stationary mean FC in Stage-2 Sleep (A) to produce a Difference Matrix (C).  $t$  tests were performed with the null hypothesis of zero correlation on the Difference Matrix (D). To correct for multiple comparisons, the false discovery rate (FDR) method was used with a  $P$  value of .01.  $t$ -tests confirmed that mean FC in Wake and Stage-2 Sleep were similar, as differences between the correlations in both conditions were not significantly greater than 0.

## 3.2 Dynamic FC

### 3.2.1 Connectivity States and Frequency

k-means clustering revealed 7 connectivity states that represent recurrent functional connectivity states in Wake and Stage-2 Sleep (**Figure 6A**). During the Wake session, 19 out of 21 participants expressed all functional connectivity states ( $M = 6.86$ ,  $SD = .48$ ); while during Stage-2 Sleep, participants expressed all connectivity states. Each connectivity state was characterized by a unique spatial topology representing a departure from mean FC. Dynamic metrics were computed from subject-specific IDX vectors separately for Wake and Stage-2 Sleep

(see **Figure 5** for examples). The effects of conditions (Wake, Stage-2 Sleep) and connectivity states on the frequency of connectivity states was examined through a Repeated Measures ANOVA (refer to **Figure 6B**). Frequency differed across connectivity states,  $F(2.63, 52.69) = 11.93, p < .001$ . There was also an effect of condition on connectivity state frequency that differed across individual states, as revealed by a significant interaction of connectivity state and condition,  $F(3.21, 64.15) = 4.57, p < .01$ . Pairwise comparisons revealed significant differences in frequency across states. Interestingly, four of seven CSs differed in the frequency of their expression across Wake and Stage-2 Sleep. Connectivity State-1 (see **Figure 6A**), which was marked by strong correlations between cortical functional families and strong anti-correlations between cortical families and subcortical networks, was more frequently expressed in Stage-2 Sleep than in Wake ( $p < .01$ ). The same was true for connectivity state-6 ( $p < .05$ ), which was marked by anti-correlations between cognitive control ICs and default mode ICs. By contrast, connectivity state-5 was more frequently expressed in Wake than Stage-2 Sleep ( $p < .01$ ), which was marked by strong positive correlations between auditory, visual, and somatomotor functional families. The same frequency of expression pattern was found for connectivity state-4 with marginal statistical significance ( $p = .053$ ) (see **Figure 6B**). Connectivity state-4 was characterized by weak positive and negative correlations, indicating a minimal departure from mean FC.

### 3.2.2 Mean Dwell Time

The effects of conditions (Wake, Stage-2 Sleep) and connectivity states on the mean dwell time of connectivity states was examined through a Repeated Measures ANOVA (refer to **Figure 6C**). Mean dwell time did not differ across connectivity states,  $F(2.12, 42.36) = .93,$



*ns*, and conditions,  $F(1) = .815$ , *ns*. There was an effect of condition on connectivity state dwell time that differed across individual states, as revealed by a significant interaction of connectivity state and condition,  $F(3, 60) = 3.56$ ,  $p < .05$ . Pairwise comparisons revealed a significant difference in the mean dwell time of connectivity state-1 indicating that participants spent more time in this state while in Stage-2 sleep than in Wake, ( $p < .05$ ) (**Figure 6C**).

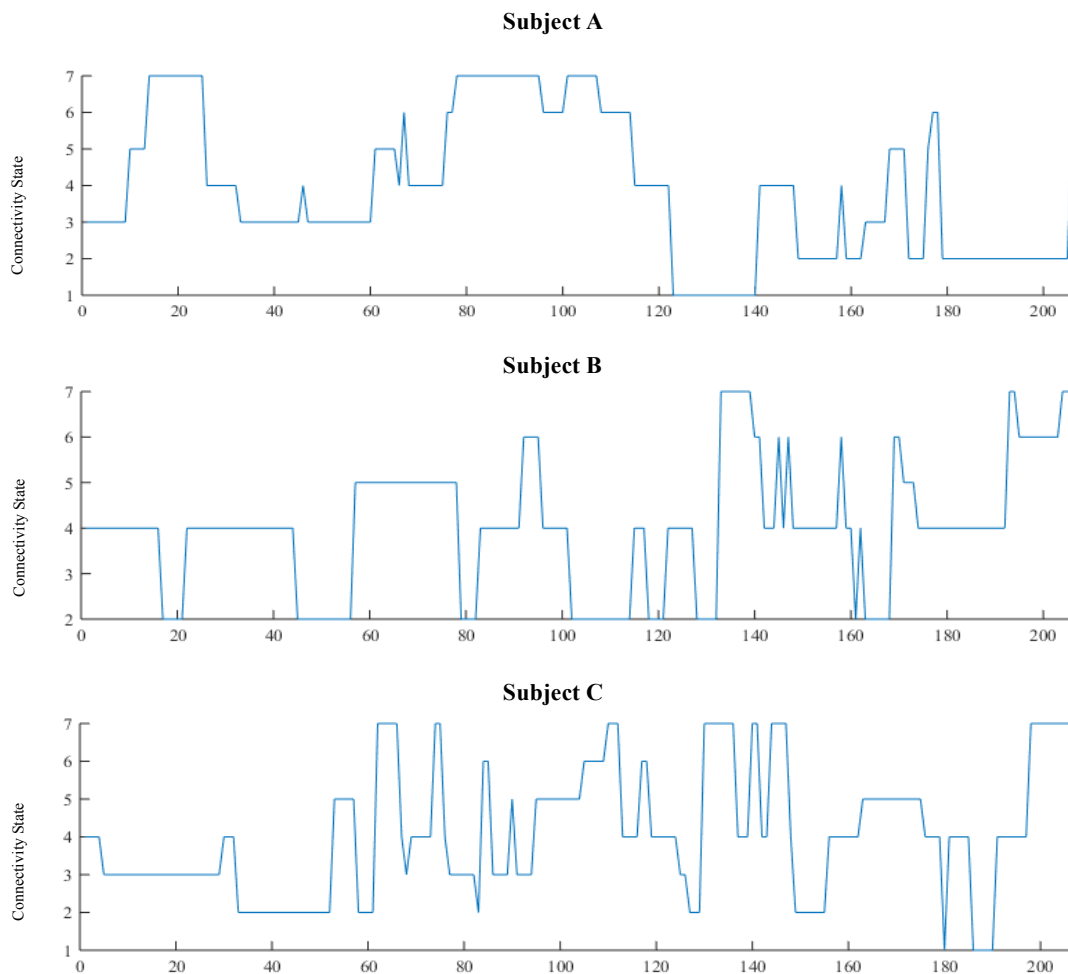


**Figure 5. IDX vector of three representative participants during wakefulness. The number of windows is on the x-axis and the connectivity state is on the y-axis. Plots illustrate**

transitions between connectivity states. The IDX vector was used to derive dynamic metrics.

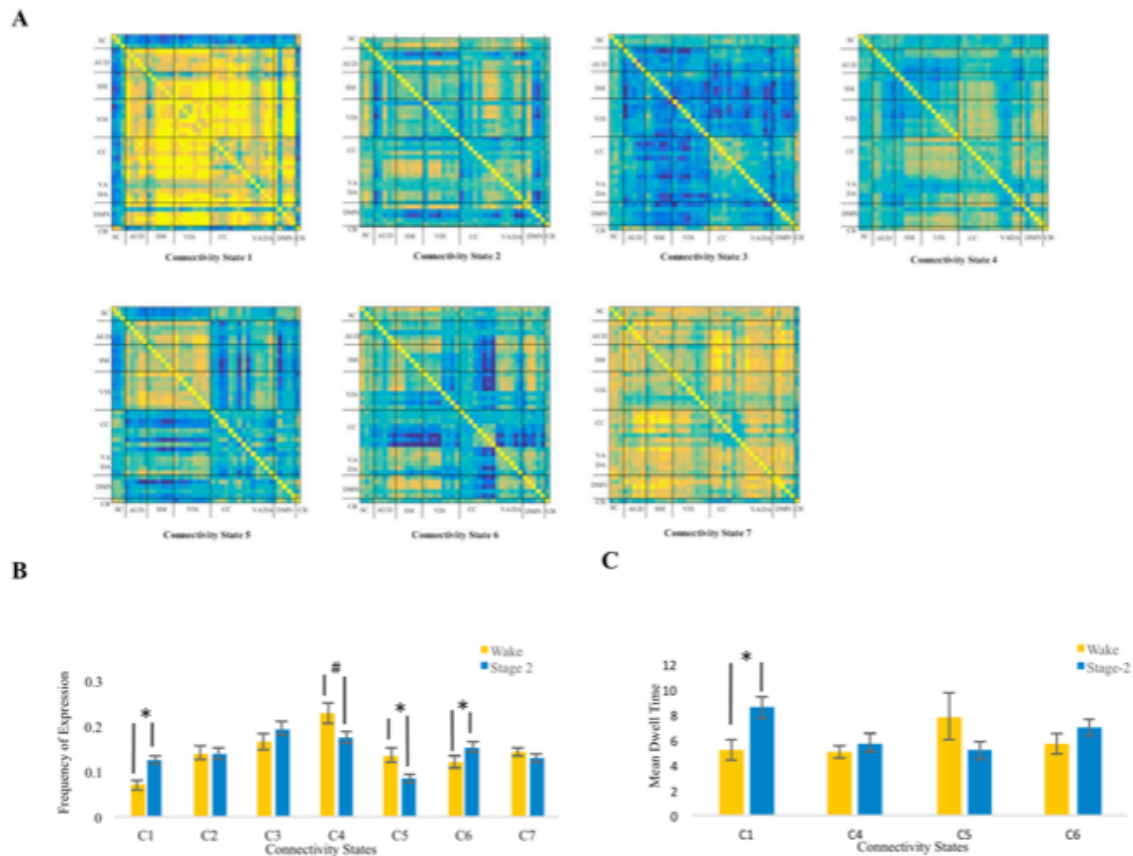


**Figure 6.** Clustering analysis revealed 7 connectivity states in Wake and Stage-2 Sleep (A). Each square represents the coupling relationship between the IC on the x-axis and the IC on the y-axis. B, mean frequency of state expression in Wake (yellow) and Stage-2 Sleep (blue). The frequency of connectivity state-1 and 6 were significantly greater in Stage-2 Sleep (\*,  $p < .05$ ). The frequency of connectivity state-5 was significantly greater in Wake (\*,  $p < .05$ ); the frequency of connectivity state-4 expression in wake was marginally significant when compared to Stage-2 Sleep (#,  $p = .053$ ). C, mean dwell time of the four connectivity states that had differences in their frequencies of expression in Wake and Stage-2 Sleep. Mean dwell time was significantly greater in Stage-2 Sleep than in Wake (\*,  $p < .05$ ).

### 3.2.3 Reliability of Connectivity States and Dynamic Metrics

Spatial correlations revealed that qualitatively similar connectivity states between varying k-solutions had the highest positive correlation. Weaker correlations between qualitatively dissimilar connectivity states were found. **Figure 7** shows spatial correlations between connectivity states derived from a k-5 and 7 solutions. Connectivity state-1 from a k-7 solution is spatially correlated ( $r = .97$ ) with its k-5 counterpart. Red dashed lines from state-1 to the other state show that the spatial correlations are weaker between dissimilar states.

Frequency of expression difference scores in connectivity state-1,-5, and -6 are not statistically significant. Difference scores shown in **Figure 8** are computed by subtracting frequencies of expression of k-15 and k-5 solutions from a k-7 solution.

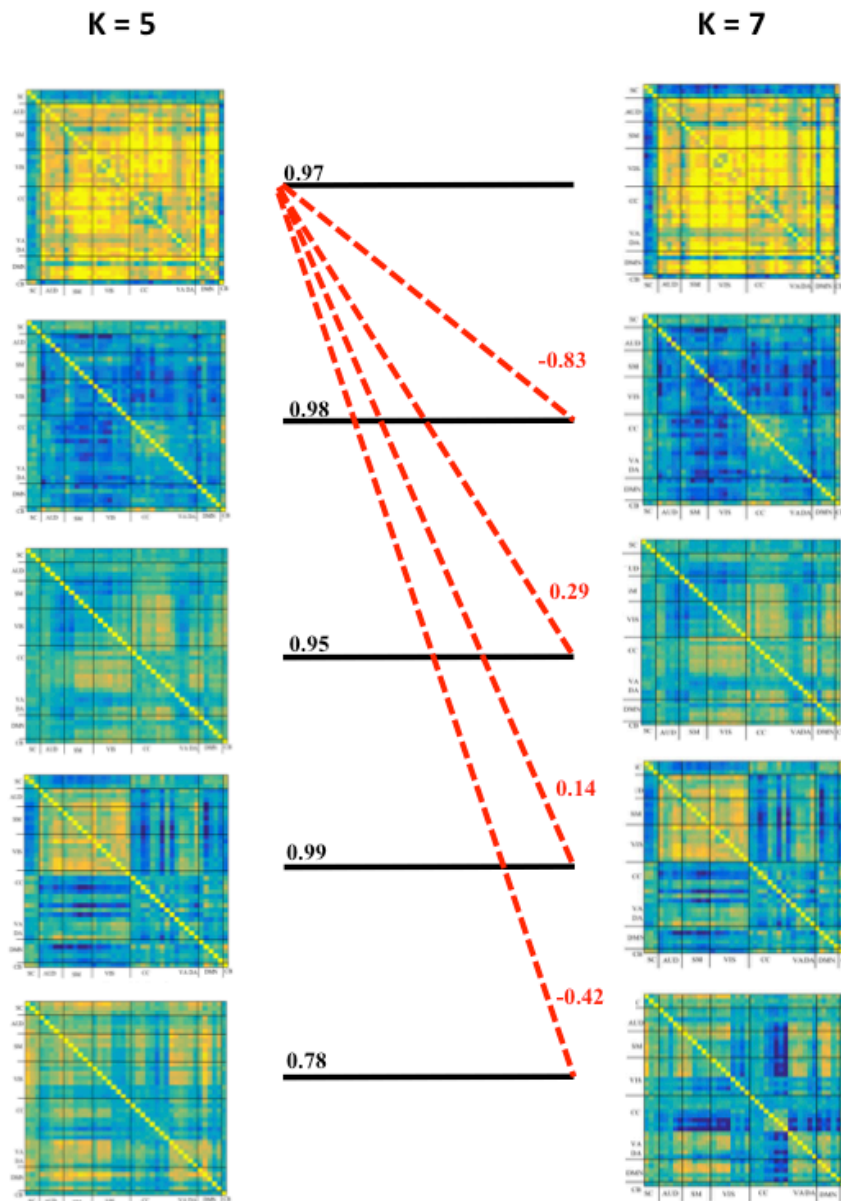


**Figure 7. Spatial correlations comparing connectivity states from a  $k=5$  solution and  $k=7$  solution. Black lines connect qualitatively similar connectivity states. Red dashed lines show the spatial correlations of connectivity state-1 in a  $k=5$  solution with connectivity states in a  $k=7$  solution. Weaker correlations are indicative of the robustness of the connectivity states in varying  $k$ -solutions and the uniqueness of their spatial topologies. Spatial correlations were iteratively computed between all connectivity states to confirm the similarity of selected connectivity states across varying  $k$ -solutions.**

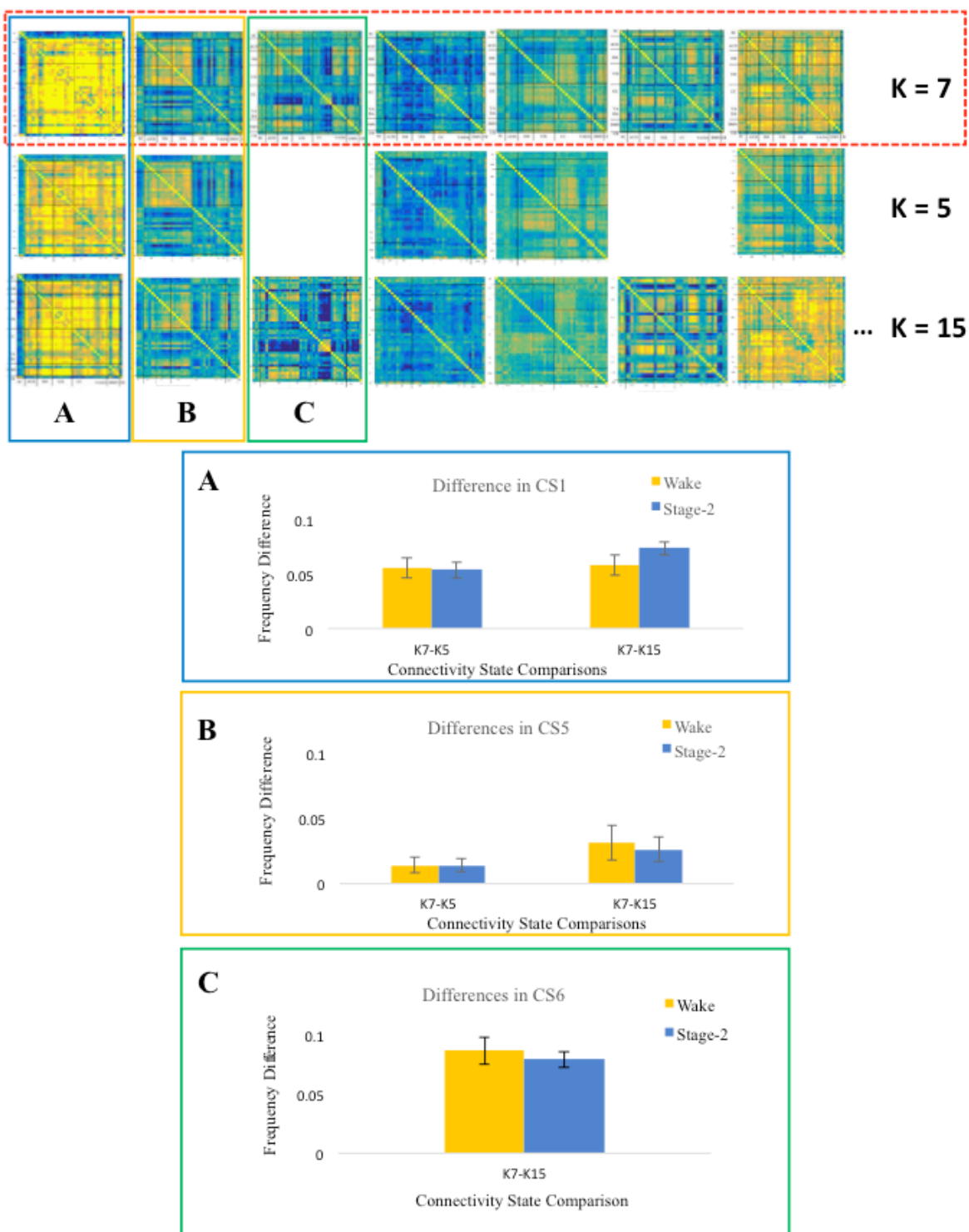


**Figure 8.** Difference scores were computed for connectivity states that showed statistically significant differences in Wake and Stage-2 Sleep. Top three panels show the connectivity states matrices derived from  $k=5$ ,  $k=7$ , and  $k=15$  solutions. The connectivity states were

organized by grouping, column-wise, qualitatively similar states. Each group is highlighted and labeled as A, B, or C. Corresponding bar graphs are also labeled and highlighted with the same colour. The frequency of expression for connectivity state-1 (A), connectivity state-5 (B), and connectivity state-6 (C) in a k5 and k15 solution was subtracted from a k7 solution frequency score. Yellow bars represent the difference scores during Wake, and blue bars represent the difference scores in Stage-2 Sleep. Frequency of expression did not change across k-solutions. This is indicative of the robustness of the dynamics analysis across different k solutions.

### 3.2.4 Temporal Characteristics of FC

Clustering analysis revealed that participants significantly transitioned more in Wake ( $M = .18$ ;  $SD = .036$ ) than in Stage-2 Sleep ( $M = .15$ ;  $SD = .033$ );  $t(20) = 2.49$ ,  $p < .05$  (**Figure 9**). Comparatively, the inter-transition interval was significantly higher in Stage-2 Sleep ( $M = 5.52$ ;  $SD = 1.10$ ) than in Wake ( $M = 7.08$ ;  $SD = 1.96$ );  $t(20) = -2.95$ ,  $p < .01$  (**Figure 10**). Therefore, average mean dwell time across connectivity states was greater in Stage-2 Sleep than in Wake.

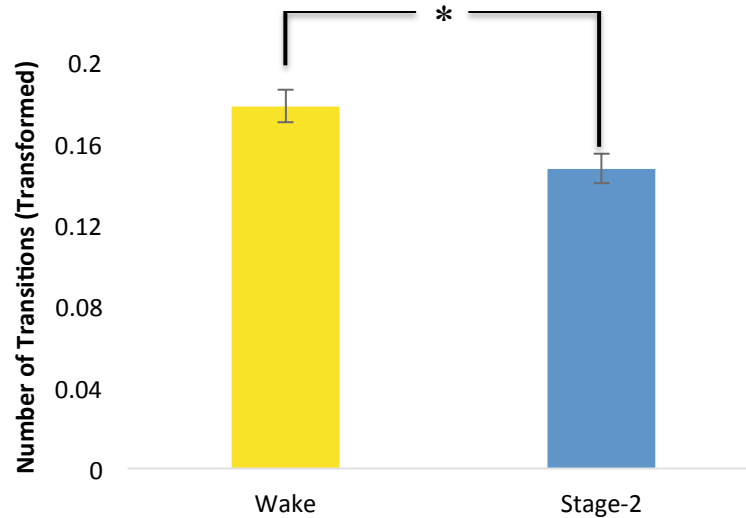


**Figure 9. Mean number of transition (NT) in Wake and Stage-2 Sleep. Participants' NTs in Wake and Stage-2 Sleep are transformed by dividing their NT by the length of their IDX vector. Participants expressed more transitions in Wake than in Stage-2 Sleep ( $p < .05$ ).**

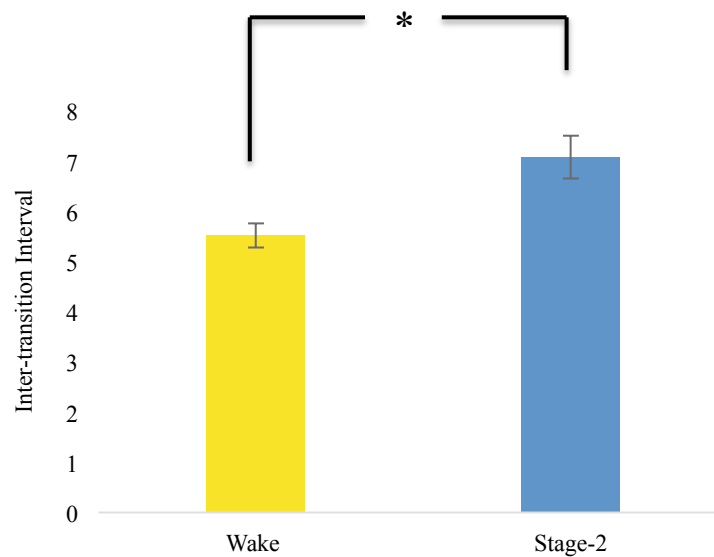


**Figure 10. Mean inter-transition interval (average number of consecutive windows) in Wake and Stage-2 Sleep. Y-axis represents the number of consecutive windows. The inter-transition interval was significantly higher in Stage-2 Sleep than in Wake ( $p < .05$ ).**

### 3.2.5 Transition Probabilities

Squares across the diagonal in each matrix (WAKE, STAGE-2 SLEEP) are marked by a hotter color (yellow), indicating a high probability of staying in a particular state (**Figure 11**). Cooler regions of the matrix, marked in blue, indicate the probability of switching between a connectivity state on the y-axis into another state on the x-axis. A difference matrix was computed by subtracting the probability matrix of Wake from the probability matrix of Stage-2 Sleep to highlight transition differences between conditions. Interestingly, the probability of staying in connectivity state-1 and connectivity state-6 was greater in Stage-2 Sleep than in Wake. This result complements aforementioned findings that show a higher frequency of expression of connectivity state 1 and 6 in Stage-2 sleep. Furthermore, the probability of transition from connectivity state-6 into 3 and from connectivity state-1 into 4 was higher in Wake than in Stage-2 Sleep.

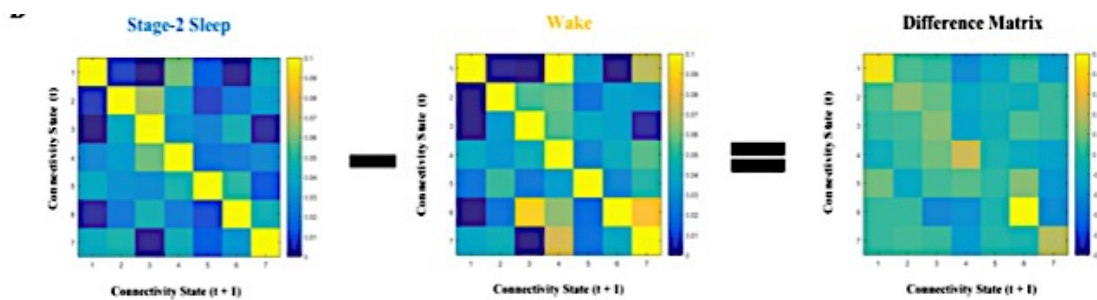


**Figure 11.** Transition probabilities for Stage-2 Sleep and Wake shown. Matrices represent the probability of transitioning from i-state on the y-axis to j-state on the x-axis. Darker yellow squares in the Difference matrix represent a higher probability of transition in Stage-2 Sleep than Wake, while darker blue squares represent a higher probability of transition in Wake than Stage-2 Sleep. Probabilities in the difference matrix range from 0 to .10.



### 3.3 Heart Rate

Participants' heart rate in Wake and Stage-2 Sleep did not significantly differ  $t(20) = 1.568$ , ns (Figure 12).

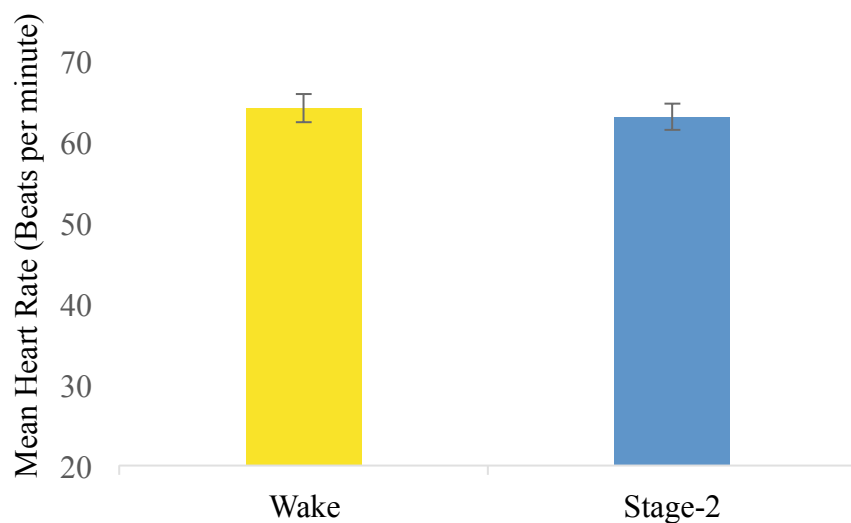


**Figure 12. Mean heart rate (beats per minute) in Wake and Stage-2 Sleep. There was no difference in heart rate between conditions.**

## 4.0 Discussion

### 4.1 Mean vs. Dynamic FC

Consistent with previous findings, there were no differences between stationary mean FC across Wake and Stage-2 Sleep (Horovitz et al., 2008; Larson-Prior et al., 2009). In both conditions, stationary mean FC matrices were marked by strong positive correlations within functional networks, and weaker positive correlations and anti-correlations between functional networks. These findings, although interesting, remain quite puzzling in light of evidence that

shows a marked change in network connectivity between wakefulness and sleep. For instance, the role of the canonical DMN has been shown as a potential mediator for conscious awareness (Boly et al., 2009; Cauda et al., 2009; Sämann et al., 2011; Tagliazucchi, von Wegner, et al., 2013). Coupling between anterior and posterior nodes of the DMN have been shown to breakdown as individuals transition from wakefulness into deep sleep (Horovitz et al., 2009). Examining spatial features of FC is important insofar as it explores changes in network connectivity across different conscious states. However, as previously reported observations suggests (Allen et al., 2017), mean FC does not fully characterize changes in FC; therefore, temporal features of FC that may differentiate between wakefulness and sleep were explored.

Given that the conventional stationary approach obscures temporal features of FC, a novel analytical method — dynamic FC (Allen et al., 2014) — was employed to reveal these features. Using dynamic methods, evidence that supports the *Slow Sleep Brain* hypothesis was found. By counting the number of transitions made between connectivity states, the brain was markedly slower while asleep than awake. Not surprisingly, slower transitions between connectivity states also impacted dwell time, as the analysis revealed longer mean dwell times across states in sleep. These findings complement previous reports showing a breakdown in effective connectivity during sleep (Massimini et al., 2005, 2010). A shift from globally integrated brain networks to disintegrated local sub-networks reduction is expected to decrease brain dynamics. Accordingly, the causal firing of neurons on the firing of other neuronal groups would translate to an increase in the average dwell time across connectivity states.

Computational models of brain function during a loss of consciousness (under sedation) show that coupling strengths between different nodes (i.e., brain regions) are weak, yet present (Deco et al., 2014; Deco, Jirsa, & McIntosh, 2013). These models delineate the stability of

spatial features of functional connections, and underscore the importance of investigating temporal features of FC (Deco et al., 2013). They highlight that temporal delays may impact the location of coupling instability without impacting the actual spatial architecture of FC (Deco et al., 2013). Given that stationary mean FC is an aggregate of all functional connections over time, these short, transient, and weak connections may be misinterpreted as absent. Stationary mean FC methods allow us to observe dominant spatial features of FC that were present in the data over time; while dynamic FC methods allows us to examine recurrent patterns of FC over time while also assessing temporal features of FC. Therefore, combining stationary and dynamic methods offers a more comprehensive view of changes in spatial and temporal features of FC across changes in conscious state, as well as, across different cognitive and behavioural states.

## 4.2 Theoretical Accounts

The slowing of the brain during sleep is instantiated in theoretical accounts that argue for a *critical* point that the brain functions at during wakefulness — a point between ordered and disordered dynamics (Petermann et al., 2009). At criticality, the brain's functional activity is governed by spatiotemporal and stochastic fluctuations that lead to multi-stable functional connectivity states (Deco, Jirsa, & McIntosh, 2011; Deco et al., 2013; Dehaene & Changeux, 2005; Ghosh, Rho, McIntosh, Kötter, & Jirsa, 2008; Hudetz, Liu, & Pillay, 2015). It has been hypothesized that these functional properties allow individuals to vigilantly attend to the external environment and access cognitive resources as needed. Indeed, there has been evidence that show support for this hypothesis by showing an association between temporal aspects of FC associated with conscious and unconscious awareness (Kucyi & Davis, 2014). In contrast, while asleep, the brain is theorized to function at sub-criticality — a point characterized by an increase

in order and decrease in flexibility (Carhart-Harris et al., 2014). Furthermore, criticality during wakefulness is analogous to goldilocks conditions, such that the brain is functioning at equilibrium — not too fast and not too slow. Therefore, based on findings presented in this thesis, it can be argued that the brain needs to dynamically and flexibly explore different functional states while awake resulting in faster and more frequent transition between connectivity states.

The criticality characterization of brain dynamics complements other theoretical work that describes the relationship between cortical entropy and consciousness (Carhart-Harris et al., 2014). Entropy is a measure of the degree of order in a system, such that a disordered state is characterized with high entropy (Carhart-Harris et al., 2014). Accordingly, the brain can be described as less entropic during sleep (i.e., increase order and more rigidity) as fewer transitions and an increase in dwell time are observed. Changes in cortical entropy has also been implicated in disorders of consciousness showing a decrease in entropy in unconscious states (Gosseries, Schnakers, & Ledoux, 2011; Sleight, Steyn-Ross, Steyn-Ross, Grant, & Ludbrook, 2004). Further, increases in cortical entropy have been observed in rats recovering from anesthesia. An increase in cortical entropy in wakefulness is also characterized by an increase in cortical information and transmission capacities, thus neural activity can be described as scale-free (Fagerholm et al., 2016). This is complementary to work that have shown that FC during wakefulness is scale-free when compared to sleep (Fagerholm et al., 2016; Lei, Wang, Yuan, & Chen, 2014). These dynamic characterizations of the brain while awake are intuitive from the standpoint of cognitive flexibility. A more entropic brain allows for more flexible and adaptive switching to meet its cognitive demands and attend to the external environment.

The transition from wakefulness to sleep has also been examined using the Hurst exponent ( $H$ ), a measure of long-term memory of time series. A marked reduction in  $H$  (towards values close to .5) has been observed during sleep compared to wakefulness indicating a reduction in long-range memory in regional time series (Tagliazucchi, von Wegner, et al., 2013). A value of  $H$  equal to .5 indicates a reduction in autocorrelation, and consequently, the potential lack of temporal correlation. An  $H$  value between .5 and 1 indicates long-range positive autocorrelations, which are interpreted as a system with increased long-range memory in regional time series. In light of presented findings, these conclusions seem contradictory and counter-intuitive given that temporal characteristics of FC slow down during sleep. An increase in  $H$  during sleep would be predicated when compared to wakefulness given that the brain is cycling less between different connectivity states, and dwelling for longer times in each state. These temporal characteristics during sleep would indicate that there is an increase in long-range memory in regional time series. However, the Hurst exponent is arguably not ideal in characterizing brain dynamics and time-series auto-correlations because the Hurst exponent is often used to examine stationary signals with a time-independent mean and variance. However, the present findings show that BOLD fluctuations are time-dependent indicating that the signal is non-stationary and thus the mean and/or the variance is not constant over time.

### 4.3 Connectivity States

The clustering approach adopted in this thesis revealed seven connectivity states that represented recurrent connectivity patterns in wakefulness and Stage-2 Sleep. Interestingly, three of the seven connectivity states had unique frequencies of expression. The selectivity of connectivity state expression is consistent with previous reports (Allen et al., 2017; Barttfeld et

al., 2015) and highlights that the transitions between different states may not be random, but due to unique differences in spatial features of FC in wakefulness and sleep. Previous reports have shown that FC patterns in awake macaques departs away from the brain's structural connectivity; comparatively, while under sedation, spatial features of FC markedly resemble the brain's structural connectivity (Barttfeld et al., 2015). A change in spatial features of FC is aligned with a spatio-temporal hypothesis that posit a change in spatial and temporal features of FC (e.g., Bharat Biswal, Zerrin Yetkin, Haughton, & Hyde, 1995; Kannurpatti et al., 2008; Pillow et al., 2008; Shmuel & Leopold, 2008). This hypothesis is grounded in the information integration theory of consciousness (Tononi, 2004; Tononi et al., 2016), that argues that spatial and temporal changes in FC mediate consciousness. Other empirical evidence that show support for spatio-temporal changes in FC due to a change in arousal stem from animal studies that employ invasive techniques such as optic and voltage imaging (Fagerholm et al., 2016; Fekete, Pitowsky, Grinvald, & Omer, 2009). For instance, an increase in arousal in primates after undergoing anesthesia is linked to an increase in the representational capacity of cortical space in the visual cortex (Fekete et al., 2009). In other words, a change in the primates' state of arousal had distinct spatial and temporal functional features that overlapped the activity space (Fekete et al., 2009). However, to definitively explore the uniqueness of the spatial features of the three aforementioned connectivity states, a direct comparison of functional connectivity and structural connectivity is needed as previously explored by Barttfeld et al. (2015).

The coupling relationships between functional networks, as observed in connectivity state-1, resemble previously reported connectivity state that was described as hypersynchronous. Cortical hypersynchrony describes the presence of strong coupling between all cortical networks (Hutchison et al., 2012). Cortical hypersynchrony is difficult to interpret given that this pattern

has been observed to be transient and short-lived (Hutchison et al., 2012). However, the hypersynchronization of the cortex may be a result of functional integration to aid in cortical synaptic plasticity (Acsády & Harris, 2017; Areal, Warby, & Mongrain, 2017) — a document effect of sleep (Acsády & Harris, 2017; Diering et al., 2017). This view is aligned with aforementioned findings given that connectivity state-1 was more frequently expressed and had a higher mean dwell time in Stage-2 Sleep than in wakefulness. Cortical hypersynchrony has been also been linked to brain plasticity in clinical settings observed in patients with Alzheimer's disease and with epilepsy (Noebels, 2011), and patients with head traumas (Santhakumar, Ratzliff, Jeng, Toth, & Soltesz, 2001; Schiff, 2006), which has been linked to brain plasticity. Therefore, temporal, and potential spatial, changes in FC may play a critical role in rewiring the brain to allow for day-to-day experience to impact brain function and development. Together, this line of evidence underscores the importance of revealing temporal changes in FC as they have the potential to supplement existing clinical biomarkers that assess consciousness (Casali et al., 2013; King et al., 2013; Sitt et al., 2014).

## 4.4 Limitations

### 4.4.1 Stationary Analysis

Stationary analysis revealed minimal qualitative differences between Wake and Stage-2 Sleep mean FC. A quantitative assessment using spatial correlation confirmed this qualitative assessment. Upon a closer look, subtle differences were detected using a difference matrix. FDR corrected ( $p < .01$ ) *t*-tests performed on the difference matrix revealed five coupling relationships between ICs that survived the correction (1 SC-VIS, 3 SM-VIS, and 1 CC-CB) (Figure 4). They do not have any obvious spatial organization that pertains to a specific functional family, or to

relationship between select functional families. The stationary analysis performed in this thesis was compressive given that it considered whole-brain ICs. The significant differences revealed, however, are hard to interpret in light of other research evidence that showed no differences between Wake and Stage-2 Sleep in specific functional networks (e.g., DMN, Horovitz et al., 2008), and whole-brain networks (Larson-Prior et al., 2009). Future research should examine these relationships in more detail on a whole-brain levels, as well as, on specific network levels.

#### 4.4.2 Dynamic Analysis

Mean dwell times of the four connectivity states discussed in this thesis are limited in their interpretation given that the analysis was selective. An omnibus statistical test was performed on the mean dwell times of four connectivity states that had significant frequency differences in wake and sleep. The selectivity of this analysis remains open to criticism because it would be expected to have differences in dwell times in states that had frequency differences in Wake and Stage-2 Sleep. However, this choice was made to minimize the number of potential pairwise comparisons made should the omnibus F-test was significant.

#### 4.4.3 Statistical Criteria

Statistical testing on the Stationary Difference Matrix was conducted on 861 comparisons, while dynamic analyses were performed on a much smaller number of comparisons (i.e., seven and four comparisons were conducted on connectivity state frequency and dwell time, respectively). Therefore, the statistical criterion used for stationary mean FC is arguable more stringent than the criterion used for dynamics analysis. For that reason, Bonferroni corrections were performed on dynamic pairwise comparisons, while FDR corrections (a less conservative approach) was performed on stationary comparisons.



## 4.5 Concluding Remarks

In conclusion, spatial changes in FC in different states of consciousness are well-documented (Boly et al., 2009; Cauda et al., 2009; Sitt et al., 2014); however, temporal features of FC have largely been ignored. In sleep and under anesthesia, a breakdown in cortical effective connectivity has been reported during the complete loss of conscious awareness (Ferrarelli et al., 2010). Temporal changes in wakefulness and sleep provide compelling evidence and a strong rationale to explore dynamic FC in patients with disorders of consciousness (e.g., patients in vegetative states). These features have the potential to be used as clinical biomarkers to assess patient's state of consciousness.

In this thesis, conventional stationary and novel dynamic methods were combined to examine changes in FC between wakefulness and sleep. The present findings provide evidence for temporal features of FC that clearly differentiate wakefulness from sleep and underscore the importance of exploring non-conventional methods to fully characterize changes in FC. These findings showed support for the *Slow Sleep Brain* hypothesis as brain dynamics were shown to slow down during sleep. The present findings corroborate previous research that have shown that functional connections are transient (Allen et al., 2014; Hutchison et al., 2012), and provide support for combining different methodologies that reveal different features of the data. Results also point towards combining imaging techniques such as fMRI and diffusion tensor imaging to answer questions pertaining to spatial and temporal relationships in different consciousness and cognitive states.

## References

- Abou-Elseoud, A., Starck, T., Remes, J., Nikkinen, J., Tervonen, O., & Kiviniemi, V. (2010). The effect of model order selection in group PICA. *Human Brain Mapping, 31*(8), 1207–1216. <http://doi.org/10.1002/hbm.20929>
- Acsády, L., & Harris, K. D. (2017). Synaptic scaling in sleep. *Science, 355*(6324). <http://doi.org/10.1126/science.aam7917>
- Albouy, G., Fogel, S., Pottiez, H., Nguyen, V. A., Ray, L., Lungu, O., ... Doyon, J. (2013). Daytime Sleep Enhances Consolidation of the Spatial but Not Motoric Representation of Motor Sequence Memory. *PLoS ONE, 8*(1), 11–13. <http://doi.org/10.1371/journal.pone.0052805>
- Allen, E. A., Damaraju, E., Plis, S. M., Erhardt, E. B., Eichele, T., & Calhoun, V. D. (2014). Tracking Whole-Brain Connectivity Dynamics in the Resting State. *Cerebral Cortex, 24*(3), 663–676. <http://doi.org/10.1093/cercor/bhs352>
- Allen, E., Eichele, T., Wu, L., & Calhoun, V. (2017). EEG Signatures of Dynamic Functional Network Connectivity States. *Brain Topography*. <http://doi.org/10.1007/s10548-017-0546-2>
- Areal, C. C., Warby, S. C., & Mongrain, V. (2017). Sleep loss and structural plasticity. *Current Opinion in Neurobiology, 44*, 1–7. <http://doi.org/10.1016/j.conb.2016.12.010>
- Barttfeld, P., Uhrig, L., Sitt, J. D., Sigman, M., & Jarraya, B. (2015). Correction for Barttfeld et al., Signature of consciousness in the dynamics of resting-state brain activity. *Proceedings of the National Academy of Sciences, 112*(37), E5219–E5220. <http://doi.org/10.1073/pnas.1515029112>

- Beck, A. T., Epstein, N., Brown, G., Steer, R. A., & others. (1988). An inventory for measuring clinical anxiety: Psychometric properties. *Journal of Consulting and Clinical Psychology*, 56(6), 893–897. <http://doi.org/10.1037/0022-006X.56.6.893>
- Beck, A. T., Steer, R. A., & Garbin, M. G. (1988). Psychometric properties of the Beck Depression Inventory: Twenty-five years of evaluation. *Clinical Psychology Review*, 8(1), 77–100. [http://doi.org/doi:10.1016/0272-7358\(88\)90050-5](http://doi.org/doi:10.1016/0272-7358(88)90050-5)
- Beck, A. T., Rial, W. Y., & Rickels, K. (1974). Short form of depression inventory: cross-validation. *Psychological Reports*.
- Biswal, B., FZ, Y., VM, H., & JS, H. (1995). - Functional connectivity in the motor cortex of resting human brain using. *Magn Reson Med*, 34(9), 537–541.  
<http://doi.org/10.1002/mrm.1910340409>
- Biswal, B., Zerrin Yetkin, F., Haughton, V. M., & Hyde, J. S. (1995). Functional connectivity in the motor cortex of resting human brain using echo-planar mri. *Magnetic Resonance in Medicine*, 34(4), 537–541. <http://doi.org/10.1002/mrm.1910340409>
- Boly, M., Perlberg, V., Marrelec, G., Schabus, M., Laureys, S., Doyon, J., ... Benali, H. (2012). Hierarchical clustering of brain activity during human nonrapid eye movement sleep. *Proceedings of the National Academy of Sciences*, 109(15), 5856–5861.  
<http://doi.org/10.1073/pnas.1111133109>
- Boly, M., Tshibanda, L., Vanhaudenhuyse, A., Noirhomme, Q., Schnakers, C., Ledoux, D., ... Laureys, S. (2009). Functional connectivity in the default network during resting state is preserved in a vegetative but not in a brain dead patient. *Human Brain Mapping*, 30(8),

2393–2400. <http://doi.org/10.1002/hbm.20672>

Carhart-Harris, R. L., Leech, R., Hellyer, P. J., Shanahan, M., Feilding, A., Tagliazucchi, E., ...

Nutt, D. (2014). The entropic brain: a theory of conscious states informed by neuroimaging research with psychedelic drugs. *Frontiers in Human Neuroscience*, 8(February), 20.

<http://doi.org/10.3389/fnhum.2014.00020>

Casali, A. G., Gosseries, O., Rosanova, M., Boly, M., Sarasso, S., Casali, K. R., ... Massimini,

M. (2013). A Theoretically Based Index of Consciousness Independent of Sensory

Processing and Behavior. *Science Translational Medicine*, 5(198), 198ra105-198ra105.

<http://doi.org/10.1126/scitranslmed.3006294>

Cauda, F., Micon, B. M., Sacco, K., Duca, S., D'Agata, F., Geminiani, G., & Canavero, S.

(2009). Disrupted intrinsic functional connectivity in the vegetative state. *Journal of Neurology, Neurosurgery, and Psychiatry*, 80(4), 429–431.

<http://doi.org/10.1136/jnnp.2007.142349>

Chang, C., & Glover, G. H. (2010). Time-frequency dynamics of resting-state brain connectivity measured with fMRI. *NeuroImage*, 50(1), 81–98.

<http://doi.org/10.1016/j.neuroimage.2009.12.011>

Chang, C., Metzger, C. D., Glover, G. H., Duyn, J. H., Heinze, H. J., & Walter, M. (2013).

Association between heart rate variability and fluctuations in resting-state functional

connectivity. *NeuroImage*, 68, 93–104. <http://doi.org/10.1016/j.neuroimage.2012.11.038>

de Pasquale, F., Della Penna, S., Snyder, A. Z., Lewis, C., Mantini, D., Marzetti, L., ... Corbetta,

M. (2010). Temporal dynamics of spontaneous MEG activity in brain networks.

*Proceedings of the National Academy of Sciences of the United States of America*, 107(13), 6040–6045. <http://doi.org/10.1073/pnas.0913863107>

de Pasquale, F., Della Penna, S., Snyder, A. Z., Marzetti, L., Pizzella, V., Romani, G. L., & Corbetta, M. (2012). A Cortical Core for Dynamic Integration of Functional Networks in the Resting Human Brain. *Neuron*, 74(4), 753–764.  
<http://doi.org/10.1016/j.neuron.2012.03.031>

Deco, G., Hagmann, P., Hudetz, A. G., & Tononi, G. (2014). Modeling resting-state functional networks when the cortex falls asleep: Local and global changes. *Cerebral Cortex*, 24(12), 3180–3194. <http://doi.org/10.1093/cercor/bht176>

Deco, G., Jirsa, V. K., & McIntosh, A. R. (2011). Emerging concepts for the dynamical organization of resting-state activity in the brain. *Nature Reviews. Neuroscience*, 12(1), 43–56. <http://doi.org/10.1038/nrn2961>

Deco, G., Jirsa, V. K., & McIntosh, A. R. (2013). Resting brains never rest: Computational insights into potential cognitive architectures. *Trends in Neurosciences*, 36(5), 268–274.  
<http://doi.org/10.1016/j.tins.2013.03.001>

Deco, G., McIntosh, A. R., Shen, K., Hutchison, R. M., Menon, R. S., Everling, S., ... Jirsa, V. K. (2014). Identification of optimal structural connectivity using functional connectivity and neural modeling. *J Neurosci*, 34(23), 7910–7916.  
<http://doi.org/10.1523/JNEUROSCI.4423-13.2014>

Dehaene, S., & Changeux, J. P. (2005). Ongoing spontaneous activity controls access to consciousness: A neuronal model for inattentive blindness. *PLoS Biology*, 3(5), 0910–

0927. <http://doi.org/10.1371/journal.pbio.0030141>

Delorme, A., & Makeig, S. (2004). EEGLAB: An open source toolbox for analysis of single-trial EEG dynamics including independent component analysis. *Journal of Neuroscience Methods*, *134*(1), 9–21. <http://doi.org/10.1016/j.jneumeth.2003.10.009>

Diekelmann, S., & Born, J. (2010). The memory function of sleep. *Nat Rev Neurosci*, *11*(2), 114–126. <http://doi.org/nrn2762> [pii]r10.1038/nrn2762

Diering, G. H., Nirujogi, R. S., Roth, R. H., Worley, P. F., Pandey, A., & Huganir, R. L. (2017). Homer1a drives homeostatic scaling-down of excitatory synapses during sleep. *Science*, *355*(February), 511–515.

Douglass, A. B., Bornstein, R., Nino-Murcia, G., Keenan, S., Miles, L., Zarcone, V. P., ... Dement, W. C. (1994). The Sleep Disorders Questionnaire. I: Creation and multivariate structure of SDQ. *Sleep*, *17*(2), 160–7. Retrieved from <http://www.ncbi.nlm.nih.gov/pubmed/8036370>

Fagerholm, E. D., Scott, G., Shew, W. L., Song, C., Leech, R., Knöpfel, T., & Sharp, D. J. (2016). Cortical Entropy, Mutual Information and Scale-Free Dynamics in Waking Mice. *Cerebral Cortex*, *26*(10), 3945–3952. <http://doi.org/10.1093/cercor/bhw200>

Fekete, T., Pitowsky, I., Grinvald, A., & Omer, D. B. (2009). Arousal increases the representational capacity of cortical tissue. *Journal of Computational Neuroscience*, *27*(2), 211–227. <http://doi.org/10.1007/s10827-009-0138-6>

Ferrarelli, F., Massimini, M., Sarasso, S., Casali, A., Riedner, B. A., Angelini, G., ... Pearce, R.

- A. (2010). Breakdown in cortical effective connectivity during midazolam-induced loss of consciousness. *Proc Natl Acad Sci U S A*, *107*(6), 2681–2686.  
<http://doi.org/10.1073/pnas.0913008107>
- Fogel, S. M., Albouy, G., Vien, C., Popovicci, R., King, B. R., Hoge, R., ... Doyon, J. (2014). fMRI and sleep correlates of the age-related impairment in motor memory consolidation. *Human Brain Mapping*, *35*(8), 3625–3645. <http://doi.org/10.1002/hbm.22426>
- Fogel, S., Ray, L. B., Binnie, L., & Owen, A. M. (2015). How to become an expert: A new perspective on the role of sleep in the mastery of procedural skills. *Neurobiology of Learning and Memory*, *125*, 236–248. <http://doi.org/10.1016/j.nlm.2015.10.004>
- Fox, M. D., & Raichle, M. E. (2007). Spontaneous fluctuations in brain activity observed with functional magnetic resonance imaging. *Nat Rev Neurosci*, *8*(9), 700–711.  
<http://doi.org/10.1038/nrn2201>
- Fox, M. D., Snyder, A. Z., Vincent, J. L., Corbetta, M., Van Essen, D. C., & Raichle, M. E. (2005). The human brain is intrinsically organized into dynamic, anticorrelated functional networks. *Proceedings of the National Academy of Sciences of the United States of America*, *102*(27), 9673–8. <http://doi.org/10.1073/pnas.0504136102>
- Fransson, P. (2005). Spontaneous low-frequency BOLD signal fluctuations: An fMRI investigation of the resting-state default mode of brain function hypothesis. *Human Brain Mapping*, *26*(1), 15–29. <http://doi.org/10.1002/hbm.20113>
- Ghosh, A., Rho, Y., McIntosh, A. R., Kötter, R., & Jirsa, V. K. (2008). Noise during rest enables the exploration of the brain's dynamic repertoire. *PLoS Computational Biology*, *4*(10).

<http://doi.org/10.1371/journal.pcbi.1000196>

Godwin, D., Barry, R. L., & Marois, R. (2015a). Breakdown of the brain's functional network modularity with awareness. *Proc Natl Acad Sci U S A*, *112*(12), 3799–3804.

<http://doi.org/10.1073/pnas.1414466112>

Godwin, D., Barry, R. L., & Marois, R. (2015b). Breakdown of the brain's functional network modularity with awareness. *Proc Natl Acad Sci U S A*, *112*(12), 3799–3804.

<http://doi.org/10.1073/pnas.1414466112>

Gosseries, O., Schnakers, C., & Ledoux, D. (2011). Automated EEG entropy measurements in coma , vegetative state / unresponsive wakefulness. *Functional Neurology*, *26*(1), 1–6.

Retrieved from <http://orbi.ulg.ac.be/handle/2268/98048>

Greicius, M. D., Krasnow, B., Reiss, A. L., & Menon, V. (2003). Functional connectivity in the resting brain: a network analysis of the default mode hypothesis. *Proceedings of the National Academy of Sciences of the United States of America*, *100*(1), 253–8.

<http://doi.org/10.1073/pnas.0135058100>

Greicius, M. D., Supekar, K., Menon, V., & Dougherty, R. F. (2009). Resting-state functional connectivity reflects structural connectivity in the default mode network. *Cerebral Cortex*, *19*(1), 72–78. <http://doi.org/10.1093/cercor/bhn059>

Hagmann, P., Cammoun, L., Gigandet, X., Meuli, R., Honey, C. J., Van Wassenhove, J., & Sporns, O. (2008). Mapping the structural core of human cerebral cortex. *PLoS Biology*, *6*(7), 1479–1493. <http://doi.org/10.1371/journal.pbio.0060159>



- Handwerker, D. A., Roopchansingh, V., Gonzalez-Castillo, J., & Bandettini, P. A. (2012). Periodic changes in fMRI connectivity Daniel. *Neuroimage*, *63*(3), 1712–1719.  
<http://doi.org/10.1038/jid.2014.371>
- Hansen, E. C. a., Battaglia, D., Spiegler, A., Deco, G., & Jirsa, V. K. (2015). Functional connectivity dynamics: Modeling the switching behavior of the resting state. *NeuroImage*, *105*, 525–535. <http://doi.org/10.1016/j.neuroimage.2014.11.001>
- Horovitz, S. G., Braun, A. R., Carr, W. S., Picchioni, D., Balkin, T. J., Fukunaga, M., & Duyn, J. H. (2009). Decoupling of the brain’s default mode network during deep sleep. *Proceedings of the National Academy of Sciences of the United States of America*, *106*(27), 11376–11381. <http://doi.org/10.1073/pnas.0901435106>
- Horovitz, S. G., Fukunaga, M., de Zwart, J. A., van Gelderen, P., Fulton, S. C., Balkin, T. J., & Duyn, J. H. (2008). Low frequency BOLD fluctuations during resting wakefulness and light sleep: A simultaneous EEG-fMRI study. *Human Brain Mapping*, *29*(6), 671–682.  
<http://doi.org/10.1002/hbm.20428>
- Hudetz, A. G., Liu, X., & Pillay, S. (2015). Dynamic Repertoire of Intrinsic Brain States Is Reduced in Propofol-Induced Unconsciousness. *Brain Connectivity*, *5*(1), 10–22.  
<http://doi.org/10.1089/brain.2014.0230>
- Hutchison, R. M., & Morton, J. B. (2015). It’s a matter of time: Reframing the development of cognitive control as a modification of the brain’s temporal dynamics. *Developmental Cognitive Neuroscience*. <http://doi.org/10.1016/j.dcn.2015.08.006>
- Hutchison, R. M., & Morton, J. B. (2015). Tracking the Brain’s Functional Coupling Dynamics

over Development. *Journal of Neuroscience*, 35(17), 6849–6859.

<http://doi.org/10.1523/JNEUROSCI.4638-14.2015>

Hutchison, R. M., Womelsdorf, T., Allen, E. a., Bandettini, P. a., Calhoun, V. D., Corbetta, M., ... Chang, C. (2013). Dynamic functional connectivity: Promise, issues, and interpretations. *NeuroImage*, 80, 360–378. <http://doi.org/10.1016/j.neuroimage.2013.05.079>

Hutchison, R. M., Womelsdorf, T., Gati, J. S., Everling, S., & Menon, R. S. (2012). Resting-state networks show dynamic functional connectivity in awake humans and anesthetized macaques. *Human Brain Mapping*, 34(9), 2154–2177. <http://doi.org/10.1002/hbm.22058>

Irwin, M. R., & Opp, M. R. (2016). Sleep-Health: Reciprocal Regulation of Sleep and Innate Immunity. *Neuropsychopharmacology*, 42(August), 1–96. <http://doi.org/10.1038/npp.2016.148>

Kannurpatti, S. S., Biswal, B. B., Kim, Y. R., & Rosen, B. R. (2008). Spatio-temporal characteristics of low-frequency BOLD signal fluctuations in isoflurane-anesthetized rat brain. *NeuroImage*, 40(4), 1738–1747. <http://doi.org/10.1016/j.neuroimage.2007.05.061>

King, J. R., Sitt, J. D., Faugeras, F., Rohaut, B., El Karoui, I., Cohen, L., ... Dehaene, S. (2013). Information sharing in the brain indexes consciousness in noncommunicative patients. *Current Biology*, 23(19), 1914–1919. <http://doi.org/10.1016/j.cub.2013.07.075>

Kirszenblat, L., & van Swinderen, B. (2015). The Yin and Yang of Sleep and Attention. *Trends in Neurosciences*, 38(12), 776–786. <http://doi.org/10.1016/j.tins.2015.10.001>

Kiviniemi, V., Starck, T., Remes, J., Long, X., Nikkinen, J., Haapea, M., ... Tervonen, O.

- (2009). Functional segmentation of the brain cortex using high model order group PICA. *Hum Brain Mapp*, 30(12), 3865–3886. <http://doi.org/10.1002/hbm.20813>
- Kiviniemi, V., Vire, T., Remes, J., Elseoud, A. A., Starck, T., Tervonen, O., & Nikkinen, J. (2011). A sliding time-window ICA reveals spatial variability of the default mode network in time. *Brain Connectivity*, 1(4), 339–347. <http://doi.org/10.1089/brain.2011.0036>
- Kucyi, A., & Davis, K. D. (2014). Dynamic functional connectivity of the default mode network tracks daydreaming. *NeuroImage*, 100, 471–480. <http://doi.org/10.1016/j.neuroimage.2014.06.044>
- Larson-Prior, L. J., Zempel, J. M., Nolan, T. S., Prior, F. W., Snyder, A. Z., & Raichle, M. E. (2009). Cortical network functional connectivity in the descent to sleep. *Proceedings of the National Academy of Sciences*, 106(11), 4489–4494. <http://doi.org/10.1073/pnas.0900924106>
- Lee, L., Harrison, L. M., & Mechelli, A. (2003). A report of the functional connectivity workshop, Dusseldorf 2002. *NeuroImage*, 19(2), 457–465. [http://doi.org/10.1016/S1053-8119\(03\)00062-4](http://doi.org/10.1016/S1053-8119(03)00062-4)
- Lei, X., Wang, Y., Yuan, H., & Chen, A. (2014). Brain Scale-free Properties in Awake Rest and NREM Sleep: A Simultaneous EEG/fMRI Study. *Brain Topography*, 28(2), 292–304. <http://doi.org/10.1007/s10548-014-0399-x>
- Lloyd, S. P. (1982). Least Squares Quantization in PCM. *IEEE Transactions on Information Theory*, 28(2), 129–137. <http://doi.org/10.1109/TIT.1982.1056489>

- Luyster, F. S., Strollo, P. J., Zee, P. C., Walsh, J. K., & Boards of Directors of the American Academy of Sleep Medicine and the Sleep Research Society. (2012). Sleep: A Health Imperative. *Sleep*, *35*(6), 727–734. <http://doi.org/10.5665/sleep.1846>
- Maingret, N., Girardeau, G., Todorova, R., Goutierre, M., & Zugaro, M. (2016). Hippocampocortical coupling mediates memory consolidation during sleep. *Nat Neurosci*, *19*(7), 959–964.  
<http://doi.org/10.1038/nn.4304>  
<http://www.nature.com/neuro/journal/v19/n7/abs/nn.4304.html#supplementary-information>
- Massimini, M., Ferrarelli, F., Huber, R., Esser, S. K., Singh, H., & Tononi, G. (2005). Breakdown of cortical effective connectivity during sleep. *Science*, *309*(5744), 2228–2232.  
<http://doi.org/10.1126/science.1117256>
- Massimini, M., Ferrarelli, F., Murphy, M. J., Huber, R., Riedner, B. A., Casarotto, S., & Tononi, G. (2010). Cortical reactivity and effective connectivity during REM sleep in humans REM sleep in humans. *Cognitive Neuroscience*, *1*(3), 176–183.  
<http://doi.org/10.1080/17588921003731578>
- Multert, C., & Lemieux, L. (2009). EEG-fMRI; Physiological Basis, Technique, and Applications. *Book*, 538. <http://doi.org/10.1007/978-3-540-87919-0>
- Noebels, J. (2011). A perfect storm: Converging paths of epilepsy and Alzheimer’s dementia intersect in the hippocampal formation. *Epilepsia*, *52*(SUPPL. 1), 39–46.  
<http://doi.org/10.1111/j.1528-1167.2010.02909.x>
- Papachristou, C. S. (2014). Aristotle’s Theory of “Sleep and Dreams” in the light of Modern and

Contemporary Experimental Research.

- Petermann, T., Thiagarajan, T. C., Lebedev, M. A., Nicolelis, M. A. L., Chialvo, D. R., & Plenz, D. (2009). Spontaneous cortical activity in awake monkeys composed of neuronal avalanches. *Proceedings of the National Academy of Sciences of the United States of America*, *106*(37), 15921–6. <http://doi.org/10.1073/pnas.0904089106>
- Pillow, J. W., Shlens, J., Paninski, L., Sher, A., Litke, A. M., Chichilnisky, E. J., & Simoncelli, E. P. (2008). Spatio-temporal correlations and visual signalling in a complete neuronal population. *Nature*, *454*(7207), 995–9. <http://doi.org/10.1038/nature07140>
- Poe, G. R. (2017). Sleep Is for Forgetting, *37*(3), 464–473.  
<http://doi.org/10.1523/JNEUROSCI.0820-16.2017>
- Raichle, M. E., & Mintun, M. A. (2006). Brain Work and Brain Imaging. *Annual Review of Neuroscience*, *29*(1), 449–476. <http://doi.org/10.1146/annurev.neuro.29.051605.112819>
- Ray, L., Sockeel, S., Soon, M., Bore, A., Myhr, A., Stojanoski, B., ... Fogel, S. M. (2015). Expert and crowd-sourced validation of an individualized sleep spindle detection method employing complex demodulation and individualized normalization. *Frontiers in Human Neuroscience*, *9*(507), 1–16. <http://doi.org/10.3389/fnhum.2015.00507>
- Rissman, J., Gazzaley, A., & D'Esposito, M. (2004). Measuring functional connectivity during distinct stages of a cognitive task. *NeuroImage*, *23*(2), 752–763.  
<http://doi.org/10.1016/j.neuroimage.2004.06.035>
- Rogers, B. P., Morgan, V. L., Newton, A. T., & Gore, J. C. (2007). Assessing functional

- connectivity in the human brain by fMRI. *Magnetic Resonance Imaging*, 25(10), 1347–1357. <http://doi.org/10.1016/j.mri.2007.03.007>
- Sämman, P. G., Wehrle, R., Hoehn, D., Spoormaker, V. I., Peters, H., Tully, C., ... Czisch, M. (2011). Development of the brain's default mode network from wakefulness to slow wave sleep. *Cerebral Cortex*, 21(9), 2082–2093. <http://doi.org/10.1093/cercor/bhq295>
- Santhakumar, V., Ratzliff, A. D. H., Jeng, J., Toth, Z., & Soltesz, I. (2001). Long-term hyperexcitability in the hippocampus after experimental head trauma. *Annals of Neurology*, 50(6), 708–717. <http://doi.org/10.1002/ana.1230>
- Schiff, N. D. (2006). Measurements and models of cerebral function in the severely injured brain. *Journal of Neurotrauma*, 23(10), 1436–49. <http://doi.org/10.1089/neu.2006.23.1436>
- Schroter, M. S., Spoormaker, V. I., Schorer, a., Wohlschlager, a., Czisch, M., Kochs, E. F., ... Ilg, R. (2012). Spatiotemporal Reconfiguration of Large-Scale Brain Functional Networks during Propofol-Induced Loss of Consciousness. *Journal of Neuroscience*, 32(37), 12832–12840. <http://doi.org/10.1523/JNEUROSCI.6046-11.2012>
- Shmuel, A., & Leopold, D. A. (2008). Neuronal correlates of spontaneous fluctuations in fMRI signals in monkey visual cortex: Implications for functional connectivity at rest. *Human Brain Mapping*, 29(7), 751–761. <http://doi.org/10.1002/hbm.20580>
- Silber, M. H., Ancoli-Israel, S., Bonnet, M. H., Chokroverty, S., Grigg-Damberger, M. M., Hirshkowitz, M., ... Iber, C. (2007). The visual scoring of sleep in adults. *Journal of Clinical Sleep Medicine*, 3(2), 121–131.

- Sitt, J. D., King, J. R., El Karoui, I., Rohaut, B., Faugeras, F., Gramfort, A., ... Naccache, L. (2014). Large scale screening of neural signatures of consciousness in patients in a vegetative or minimally conscious state. *Brain*, *137*(8), 2258–2270. <http://doi.org/10.1093/brain/awu141>
- Sleigh, J. W., Steyn-Ross, D. A., Steyn-Ross, M. L., Grant, C., & Ludbrook, G. (2004). Cortical entropy changes with general anaesthesia: theory and experiment. *Physiological Measurement*, *25*(4), 921–934. <http://doi.org/10.1088/0967-3334/25/4/011>
- Smith, S. M., Fox, P. T., Miller, K. L., Glahn, D. C., Fox, P. M., Mackay, C. E., ... Beckmann, C. F. (2009). Correspondence of the brain's functional architecture during activation and rest. *Proceedings of the National Academy of Sciences of the United States of America*, *106*(31), 13040–5. <http://doi.org/10.1073/pnas.0905267106>
- Smith, S. M., Miller, K. L., Moeller, S., Xu, J., Auerbach, E. J., Woolrich, M. W., ... Ugurbil, K. (2012). Temporally-independent functional modes of spontaneous brain activity. *Proceedings of the National Academy of Sciences of the United States of America*, *109*(8), 3131–6. <http://doi.org/10.1073/pnas.1121329109>
- Spoormaker, V. I., Gleiser, P. M., & Czigic, M. (2012). Frontoparietal connectivity and hierarchical structure of the brain's functional network during sleep. *Frontiers in Neurology*, *MAY*(May), 1–10. <http://doi.org/10.3389/fneur.2012.00080>
- Spoormaker, V. I., Schröter, M. S., Gleiser, P. M., Andrade, K. C., Dresler, M., Wehrle, R., ... Czigic, M. (2010). Development of a Large-Scale Functional Brain Network during Human Non-Rapid Eye Movement Sleep. *J. Neurosci.*, *30*(34), 11379–11387.

<http://doi.org/10.1523/JNEUROSCI.2015-10.2010>

Tagliazucchi, E., Balenzuela, P., Fraiman, D., & Chialvo, D. R. (2012). Criticality in large-scale brain fmri dynamics unveiled by a novel point process analysis. *Frontiers in Physiology*, 3 FEB(February), 1–12. <http://doi.org/10.3389/fphys.2012.00015>

Tagliazucchi, E., Behrens, M., & Laufs, H. (2013). Sleep neuroimaging and models of consciousness. *Frontiers in Psychology*, 4(MAY), 1–9. <http://doi.org/10.3389/fpsyg.2013.00256>

Tagliazucchi, E., Crossley, N., Bullmore, E. T., & Laufs, H. (2016). Deep sleep divides the cortex into opposite modes of anatomical-functional coupling. *Brain Structure and Function*, 221(8), 4221–4234. <http://doi.org/10.1007/s00429-015-1162-0>

Tagliazucchi, E., von Wegner, F., Morzelewski, A., Borisov, S., Jahnke, K., & Laufs, H. (2012). Automatic sleep staging using fMRI functional connectivity data. *NeuroImage*, 63(1), 63–72. <http://doi.org/10.1016/j.neuroimage.2012.06.036>

Tagliazucchi, E., von Wegner, F., Morzelewski, A., Brodbeck, V., Jahnke, K., & Laufs, H. (2013). Breakdown of long-range temporal dependence in default mode and attention networks during deep sleep. *Proceedings of the National Academy of Sciences of the United States of America*, 110(31), 15419–24. <http://doi.org/10.1073/pnas.1312848110>

Tagliazucchi, E., Wegner, F. Von, Morzelewski, A., Brodbeck, V., Laufs, H., von Wegner, F., ... Laufs, H. (2012). Dynamic BOLD functional connectivity in humans and its electrophysiological correlates. *Frontiers in Human Neuroscience*, 6(December), 339. <http://doi.org/10.3389/fnhum.2012.00339>



- Tononi, G. (2004). An information integration theory of consciousness. *BMC Neuroscience*, 5, 42–64. <http://doi.org/10.1186/1471-2202-5-42>
- Tononi, G., Boly, M., Massimini, M., & Koch, C. (2016). Integrated Information Theory: from consciousness to its physical substrates. *Nature Reviews Neuroscience*, *in press*(7), 450–461. <http://doi.org/10.1038/nrn.2016.44>
- Tononi, G., & Cirelli, C. (2014). Sleep and the Price of Plasticity: From Synaptic and Cellular Homeostasis to Memory Consolidation and Integration. *Neuron*, 81(1), 12–34. <http://doi.org/10.1016/j.neuron.2013.12.025>
- Vincent, J. L., Patel, G. H., Fox, M. D., Snyder, A. Z., Baker, J. T., Van Essen, D. C., ... Raichle, M. E. (2007). Intrinsic functional architecture in the anaesthetized monkey brain. *Nature*, 447(7140), 83–86. <http://doi.org/10.1038/nature05758>
- Xie, L., Kang, H., Xu, Q., Chen, M. J., Liao, Y., Thiyagarajan, M., ... Nedergaard, M. (2013). Sleep Drives Metabolite Clearance from the Adult Brain. *Science*, 342, 373–377. <http://doi.org/10.1126/science.1241224>
- Yang, G., Lai, C. S. W., Cichon, J., Ma, L., Li, W., & Gan, W.-B. (2014). Sleep promotes branch-specific formation of dendritic spines after learning. *Science*, 344(6188), 1173–1178.

## Curriculum Vitae

**Name:** Mazen El-Baba

**Post-secondary Education and Degrees:** University of Guelph  
Guelph, Ontario, Canada  
2011-2015 BSc.

The University of Western Ontario  
London, Ontario, Canada  
2015-2017 MSc. Candidate

**Honours and Awards:** **Alexander Graham Bell Canada Graduate Scholarship, \$17,500**  
2016-2017

**SSHRC Partnership Grant, \$2.5M**  
**Child and Youth Refugee Research Coalition**  
Collaborator  
2017-2019

**Social Science Internal Fund, \$8,000**  
2017

**SSHRC Insight Grant, \$210,989**  
Cowriter  
2016-2018

**Canada Service Summer Grant**  
**2017, \$54,500**  
**2016, \$35,595**

**Province of Ontario Graduate Scholarship, \$15,000**  
2015-2016  
2016-2017 (declined)

**Neuroscience Travel Award, \$500**  
2017

**McGill Recruitment Award, \$3,000**  
2015-2016 (*declined*)

**Community Service Award, \$500**  
2016

**Volunteerism Awards**

Ghana Medical Help, 2013, 2014  
Best Buddies Program 2010, 2011

**Awards of Excellence**

Student Housing, University of Guelph, 2012, 2013, 2014, 2015

**Related Work  
Experience**

**Teaching Assistant**

The University of Western Ontario  
Research in Developmental Psychology (3485)  
Biology for Science II (1000)  
Research in Developmental Cognitive Neuroscience (3480)  
Developmental Cognitive Neuroscience (3440)  
2015-2017

**Research Coordinator**

Ghana Medical Help  
Sandema Ghana & Toronto Canada  
2013-2016

**Research Assistant**

Cognitive Development and Neuroimaging Laboratory  
Western University  
2015

**Research Assistant**

Leri Lab  
University of Guelph  
2013-2014

**Research Assistant**

Environment and Land Tribunal Ontario (ELTO)  
Ministry of Attorney General  
Toronto, Ontario  
2013

**Publications:**

**El-Baba, M.** Lateral Prefrontal Cortex. Encyclopedia of Personality and Individual Differences. Springer Encyclopaedia. (2017).